

# INCREASING AND DECREASING SEQUENCES IN FILLINGS OF MOON POLYOMINOES

MARTIN RUBEY

ABSTRACT. We present an adaptation of *jeu de taquin* and promotion for arbitrary fillings of moon polyominoes. Using this construction we show various symmetry properties of such fillings taking into account the lengths of longest increasing and decreasing chains. In particular, we prove a conjecture of Jakob Jonsson. We also relate our construction to the one recently employed by Christian Krattenthaler, thus generalising his results.

## 1. INTRODUCTION

This article exploits properties of *jeu de taquin*, promotion and evacuation, extended to fillings of matrices with non-negative integer entries. Our principal motivation was to prove a conjecture due to Jakob Jonsson [12], which is Theorem 5.1 of this article. In rough terms, this theorem states that the number of fillings with zeros and ones of a given moon polyomino (see Definition 2.2) that do not contain a north-east chain of non-zero entries longer than a given threshold (see Definition 2.2) only depends on the distribution of heights of the columns of the polyomino. Aesthetics aside, one of the reasons to consider this theorem is that for polyominoes of certain shapes the number of such fillings is much easier to count than for others.

Jakob Jonsson's starting point was the desire to count generalised triangulations with a given size of a maximal crossing. He related these objects to fans of Dyck paths, which were already counted by Myriam de Sainte-Catherine and Xavier Viennot [6].

As Christian Krattenthaler [15] noticed, Jakob Jonsson's observation can be seen as a generalisation of symmetry properties of sizes of maximal crossings and nestings in matchings and set-partitions. These have been proved a little earlier by William Chen, Eva Deng, Rosena Du, Richard Stanley and Catherine Yan [3], using the Robinson-Schensted algorithm. In my opinion, Christian Krattenthaler's most important contribution was to prove these statements – and generalisations thereof – using Sergey Fomin's growth diagrams [8, 9, 10, 18].

Curiously, all we use in this article are well known tools, although it seems that some of their properties we need went unnoticed so far. In particular, Proposition 4.7 states a locality property of promotion and the Robinson-Schensted-Knuth algorithm that might be interesting in its own right. A weaker form of this property has been used by Astrid Reifegerste [17] to deduce the sign of a permutation directly from the pair of tableaux associated to it via the Robinson-Schensted correspondence.

Meanwhile at least two articles dealing with other properties of fillings of moon polyominoes have appeared. In particular, Anisse Kasraoui [14] found that the

---

*Key words and phrases.* *jeu de taquin*, promotion, evacuation, plactic monoid, growth diagrams, moon polyominoes, L-convex polyominoes, crossings and nestings.

Research partially supported by the Austrian Science Foundation FWF, grant S9607-N13, in the framework of the National Research Network “Analytic Combinatorics and Probabilistic Number Theory”.

number of north-east and south-east chains of length two in 0-1-fillings of a moon polyomino remains invariant if the columns of the polyomino are permuted, given that the result is again a moon polyomino, and there is at most one non-zero entry in every column. Very remarkably, Anisse Kasraoui even found an astonishingly simple expression for the generating function counting the number of such fillings.

William Chen, Svetlana Poznanović, Catherine Yan and Arthur Yang [4] defined a major index for fillings of 0-1-fillings, that specialises to the major index for words and permutations when the polyomino is a rectangle, and to the major index for matchings and set partitions when the polyomino is a Ferrers shape. Again, this major index is invariant under permutations of the columns of the moon polyomino, when the result is a moon polyomino. Moreover, they found that the generating function for their major index coincides with the one given by Anisse Kasraoui.

In this article, we used the growth diagram description of the Robinson-Schensted algorithm, and its Greene invariant that encodes in particular the length of the longest north-east chain in the filling. At least for Theorem 5.3, that deals with arbitrary fillings, an analogous theorem should hold for any Greene invariant of a pair of dual-graded graphs, where a promotion operator is available. For example, we could take as pair of dual graded graphs the lifted binary tree and the graph associated to binary words, as in Section 4.6 of Sergey Fomin's article [10]. The resulting statistic on the fillings is then the maximal number of descents (i.e., north-west chains of length two in consecutive rows) in a rectangle. Of course, the details have yet to be worked out, but there is certainly a lot more to come.

**Acknowledgements.** This article has undergone substantial changes since its first version, and I would like to thank those who made this final version possible. First of all however I need to thank Christian Krattenthaler for presenting the problem in the Arbeitsgemeinschaft Diskrete Mathematik, and then my wife Anita for creating an atmosphere that let me have the crucial ideas during January 2006. I feel indebted to several anonymous referees who made me check all my proofs and thus discover (and fix!) many little and not so little gaps. Last but not least, I'm very grateful for the patience of éditrice Mireille Bousquet-Mélou, and for constant support and interest of many colleagues.

## 2. DEFINITIONS

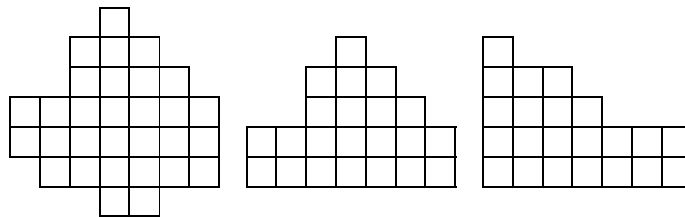


FIGURE 1. a moon-polyomino, a stack-polyomino and a Ferrers diagram

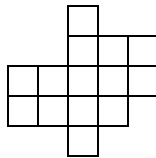
### 2.1. Polyominoes.

**Definition 2.1.** A *polyomino* is a finite subset of  $\mathbb{Z}^2$ , where we regard an element of  $\mathbb{Z}^2$  as a cell. A *column* of a polyomino is the set of cells along a vertical line, a *row* is the set of cells along a horizontal line.

The polyomino is *convex*, if for any two cells in a column, the elements of  $\mathbb{Z}^2$  in between are also cells of the polyomino, and for any two cells in a row, the elements of  $\mathbb{Z}^2$  in between are also cells of the polyomino. It is *intersection-free*, if any two

columns are *comparable*, i.e., the set of row coordinates of cells in one column is contained in the set of row coordinates of cells in the other. Equivalently, it is intersection-free, if any two rows are comparable.

For example, the polyomino



is convex, but not intersection-free, since the first and the last columns are incomparable.

**Definition 2.2.** A *moon polyomino* is a convex, intersection-free polyomino. A *stack polyomino* is a moon-polyomino if all columns start at the same level. A *Ferrers diagram* is a stack-polyomino with weakly decreasing row widths  $\lambda_1, \lambda_2, \dots, \lambda_n$ , reading rows from bottom to top. We alert the reader that we are using ‘French’ notation for Ferrers diagrams.

For a permutation  $\sigma$  of the column indices of a moon polyomino  $M$ , *reordering the columns according to  $\sigma$*  yields the polyomino  $\sigma M = \{(\sigma i, j) : (i, j) \in M\}$ . Thus, the columns are only translated horizontally and keep their vertical offsets.

The *content* of a moon polyomino is the sequence of column heights, in decreasing order. For example, the content of the moon polyomino at the left of Figure 1 is  $(7, 6, 5, 4, 3, 3, 2)$ , while the content of the other two polyominoes in the same figure is  $(5, 4, 4, 3, 2, 2, 2)$ .

*Remark.* The name ‘moon polyomino’ was used by Jakob Jonsson in [12]. Curiously, this class of polyominoes was independently introduced a little earlier by Giusi Castiglione and Antonio Restivo [2] as *L-convex* (or, alternatively *1-convex*) polyominoes. The defining property they use is that every pair of cells can be connected by a path consisting of horizontal and vertical steps that changes direction at most once.

## 2.2. Fillings and Chains.

**Definition 2.3.** An *arbitrary filling* of a polyomino is an assignment of natural numbers to the cells of the polyomino. We refer to the number in a cell as the *multiplicity* of the entry.

In a *0-1-filling* we restrict ourselves to the numbers 0 and 1. A *standard filling* has the additional constraint that in each column and in each row there is exactly one entry 1, whereas a *partial filling* has at most one entry 1 in each column and in each row.

*Remark.* In the figures, we will usually omit zeros, and in 0-1-fillings we will replace ones by crosses for aesthetic reasons. We reserve the letters  $\alpha, \beta, \gamma, \delta, \epsilon$  and  $\pi$  to denote fillings.

**Definition 2.4.** A *chain* is a sequence of non-zero entries in a filling such that the smallest rectangle containing all its elements of the sequence is completely contained in the moon polyomino.

A *north-east chain*, or short *ne-chain* of length  $k$  in an arbitrary filling of a moon polyomino is a chain of  $k$  non-zero entries, such that each element is strictly to the right and strictly above the preceding element of the sequence. Similarly, in a *south-east chain*, for short *se-chain*, each element is strictly to the right and strictly below the preceding element. The length of such a chain is the number of its elements.

*NE-chains* and *SE-chains* may have elements in the same column and in the same row. For these kinds of chains, each element contributes its multiplicity to the length. That is, a *NE-chain* of length  $k$  is a chain such that each element is weakly to the right and weakly above its predecessor, and the sum of the multiplicities of the elements equals  $k$ .

For 0-1-fillings we also define *nE-chains* and *sE-chains*, where we allow an element of the chain to be in the same column as its predecessor, but not in the same row. Similarly, elements of *Ne-chains* and *Se-chains* are allowed to be in the same row, but not in the same column.

For example, consider the following two fillings:

$$\begin{array}{|c|c|c|} \hline & & 1 \\ \hline & 1 & 3 \\ \hline 3 & & 1 \\ \hline 1 & 1 & \\ \hline \end{array}
 \quad \text{and} \quad
 \begin{array}{|c|c|c|} \hline & & 1 \\ \hline & 1 & \\ \hline & & 1 \\ \hline & 1 & \\ \hline \end{array}$$

The length of the longest ne-chain in the filling on the left is three, whereas the length of the longest se-chain is two. The lengths of the longest NE- and SE-chains are six and five respectively.

The lengths of the longest nE-, Ne-, sE-, and Se-chains in the 0-1-filling on the right are four, two, three and one respectively.

### 2.3. Partitions and Tableaux.

**Definition 2.5.** A *partition* is a weakly decreasing sequence of natural numbers, which are called its *parts*. The *length* of a partition is the number of its parts, the *size* of a partition is the sum of its parts. A partition  $\lambda = (\lambda_1, \lambda_2, \dots, \lambda_l)$  is *contained* in another partition  $\mu = (\mu_1, \mu_2, \dots, \mu_m)$  if  $l \leq m$  and  $\lambda_i \leq \mu_i$  for all  $i \leq l$ .

The union of  $\lambda$  and  $\mu$ , denoted  $\lambda \cup \mu$ , is the partition  $\kappa = (\kappa_1, \kappa_2, \dots, \kappa_k)$  with  $k = \max(l, m)$  and  $\kappa_i = \max(\lambda_i, \mu_i)$  for all  $i \leq k$ , where we set  $\lambda_i = 0$  for  $i > l$  and  $\mu_i = 0$  for  $i > m$ .

The *transpose* or *conjugate* of a partition  $\lambda$  is defined as  $\lambda^t = (\mu_1, \mu_2, \dots, \mu_m)$ , where  $m = \lambda_1$  and  $\mu_i$  is the number of parts in  $\lambda$  greater than or equal to  $i$ .

The *transpose* of a sequence of partitions  $P = (\emptyset = \lambda^0, \lambda^1, \dots, \lambda^n)$  is the sequence of partitions  $P^t$  obtained by transposing each individual partition.

*Remark.* A Ferrers shape (in French notation) corresponds to a partition  $\lambda$ , setting  $\lambda_i$  to the length of the  $i^{\text{th}}$  row from bottom to top. Using this correspondence, the transpose of a partition can be obtained by reflecting the corresponding Ferrers shape about the main diagonal.

**Definition 2.6.** A *semi-standard Young tableau* is a filling of a Ferrers shape with positive integers, such that entries are weakly increasing in rows and strictly increasing – from bottom to top – in columns.

A *standard Young tableau* is a semi-standard Young tableau with entries being the numbers 1 through  $n$ , such that each number occurs exactly once.

A *partial Young tableau* is a semi-standard Young tableau with all entries distinct.

*Remark.* An example for a pair of standard Young tableaux is given in Equation (1). Although Young tableaux happen to be fillings of Ferrers shapes, they should be thought of as objects entirely different from the fillings introduced in Definition 2.3.

3. GROWTH DIAGRAMS AND THE ROBINSON-SCHENSTED-KNUTH CORRESPONDENCE

Sergey Fomin’s growth diagrams together with Marcel Schützenberger’s *jeu de taquin* and *promotion* will be the central tools in this article. In this section we introduce growth diagrams, which associate sequences of partitions to fillings of matrices with non-negative integer entries. Although the contents of this section is well known, we reproduce it here for the convenience of the reader. Some additional information and more references can be found in [15, Sections 2 and 4].

**3.1. Local Rules and Growth Diagrams.** Consider a rectangular polyomino with a partial filling, as, for example, in Figure 3.a where we have replaced zeros by empty cells and ones by crosses. Using the following construction we will inductively label the corners of each cell with a partition, starting from the bottom left corner, to obtain a *growth diagram*.

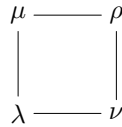


FIGURE 2. a cell of a growth diagram

First, we attach the empty partition  $\emptyset$  to the corners along the lower and the left border. Suppose now that we have already labelled all the corners of a square except the top right with partitions  $\lambda$ ,  $\mu$  and  $\nu$ , as in Figure 2. We compute  $\rho$  as follows:

- F1 Suppose that the square does not contain a cross, and that  $\lambda = \mu = \nu$ . Then set  $\rho = \lambda$ .
- F2 Suppose that the square does not contain a cross, and that  $\mu \neq \nu$ . Then set  $\rho = \mu \cup \nu$ .
- F3 Suppose that the square does not contain a cross, and that  $\lambda \subsetneq \mu = \nu$ . Then we obtain  $\rho$  from  $\mu$  by adding 1 to the  $i + 1^{\text{st}}$  part of  $\mu$ , given that  $\lambda$  and  $\mu$  differ in the  $i^{\text{th}}$  part.
- F4 Suppose that the square contains a cross. This implies that  $\lambda = \mu = \nu$  and we obtain  $\rho$  from  $\lambda$  by adding 1 to the first part of  $\lambda$ .

The important fact is, that this process is invertible: given the labels of the corners along the upper and right border of the diagram, we can reconstruct the complete growth diagram as well as the entries of the squares. To this end, suppose that we have already labelled all the corners of a square except the bottom left with partitions  $\mu$  and  $\nu$  and  $\rho$ , as in Figure 2. We compute  $\lambda$  and the entry of the square as follows:

- B1 If  $\mu = \nu = \rho$  we set  $\lambda = \rho$  and leave the square empty.
- B2 If  $\mu \neq \nu$  we set  $\lambda = \mu \cap \nu$  and leave the square empty.
- B3 If  $\mu = \nu \subsetneq \rho$  and  $\mu$  and  $\rho$  differ in the  $i^{\text{th}}$  part for  $i \geq 2$ , we obtain  $\lambda$  from  $\mu$  by deleting 1 from the  $i - 1^{\text{st}}$  part of  $\mu$  and leave the square empty.
- B4 If  $\mu = \nu \subsetneq \rho$  and  $\mu$  and  $\rho$  differ in the first part we set  $\lambda = \mu$  and mark the square with a cross.

**3.2. The Robinson-Schensted Correspondence and Greene’s Theorem.** In the case of a standard filling of a square, the sequence of partitions  $\emptyset = \mu^0, \mu^1, \dots, \mu^n$  along the upper border of the growth diagram corresponds to a standard Young tableau  $Q$  as follows: we put the entry  $i$  into the cell by which  $\mu^{i-1}$  and  $\mu^i$  differ.



Furthermore, the filling itself defines a permutation  $\pi$ . For example in Figure 3.a we have  $\pi = 6, 1, 5, 3, 7, 8, 4, 2$  and

$$(1) \quad (P, Q) = \left( \begin{array}{|c|c|c|c|} \hline 6 & & & \\ \hline 5 & & & \\ \hline 3 & 7 & & \\ \hline 1 & 2 & 4 & 8 \\ \hline \end{array}, \begin{array}{|c|c|c|c|} \hline 8 & & & \\ \hline 4 & & & \\ \hline 2 & 7 & & \\ \hline 1 & 3 & 5 & 6 \\ \hline \end{array} \right).$$

It is well known (see for example Theorem 7.13.5 of [21]) that  $Q$  is the recording and  $P$  the insertion tableau produced by the Robinson-Schensted correspondence, applied to the permutation  $\pi$ .

Since the partitions along the upper and right border of a growth diagram determine the filling and vice versa, the following definition will be useful:

**Definition 3.1.** Let  $\pi$  be a partial filling of a rectangular polyomino and consider the corresponding growth diagram. Suppose that the corners along the right border are labelled with a sequence of partitions  $P$ , and along the upper border with a sequence of partitions  $Q$ . We then say, that  $\pi$  *corresponds* to the pair  $(P, Q)$ . The last partitions of  $P$  and  $Q$  coincide, and this partition is the *shape* of the filling  $\pi$ .

For our purposes it is of great importance that the partitions appearing in the corners of a growth diagram also have a ‘global’ description. This is called *Greene’s Theorem* (due to Curtis Greene [11]):

**Theorem 3.2.** [21, Theorem A.1.1.1] *Suppose that a corner  $c$  of a growth diagram is labelled by a partition  $\lambda$ . Then, for any integer  $k$ , the maximal cardinality of a union of  $k$  pairwise disjoint north-east chains situated in the rectangular region to the left and below of  $c$  is equal to  $\lambda_1 + \lambda_2 + \dots + \lambda_k$ .*

*Furthermore, the maximal cardinality of the union of  $k$  pairwise disjoint south-east chains situated in the rectangular region to the left and below of  $c$  is equal to  $\lambda'_1 + \lambda'_2 + \dots + \lambda'_k$ , where  $\lambda'$  is the transpose of  $\lambda$ .*

*Remark.* In [21] this theorem is only stated for standard fillings. To obtain the statement for partial fillings, it suffices to observe that by rule F1 empty columns and rows can be ignored.

**3.3. Variations of the Robinson-Schensted-Knuth Correspondence.** In the following we extend the construction described in Section 3.1 to arbitrary fillings of rectangular polyominoes. We construct a new diagram with more rows and columns, and place non-zero entries which are originally in the same column or row in different columns and rows in the larger diagrams. A similar strategy is applied to entries with multiplicity larger than one. We refer to this process, transforming a filling  $\pi$  into a standard filling  $std(\pi)$ , as *standardisation*. More precisely, we proceed as follows:

**3.3.1. First Variant: RSK.** Each row and each column of the original diagram is replaced by as many rows and columns in the new diagram as it contains non-zero entries, counting multiplicities. Then, for each row and for each column of the original diagram we place the non-zero entries into the new diagram as a north-east chain. An example can be found in Figure 4, the result being the left of the two standardised diagrams. Note that this process preserves the length of the NE- and se-chains.

Given a filling  $\pi$ , we can apply the rules F1 to F4 to the transformed diagram and obtain a pair of sequences of partitions  $(\bar{P}, \bar{Q})$  with  $\bar{P} = (\emptyset = \bar{\lambda}^0, \bar{\lambda}^1, \dots, \bar{\lambda}^n)$  and  $\bar{Q} = (\emptyset = \bar{\mu}^0, \bar{\mu}^1, \dots, \bar{\mu}^n)$ . The sequences of partitions corresponding to the original diagram are then given by  $P = (\emptyset = \lambda^0, \lambda^1, \dots, \lambda^k)$  and  $Q = (\emptyset = \mu^0, \mu^1, \dots, \mu^k)$  with  $\lambda^i = \bar{\lambda}^{\#\text{non-zero entries below row } i}$  and  $\mu^i = \bar{\mu}^{\#\text{non-zero entries left of column } i}$ . Less

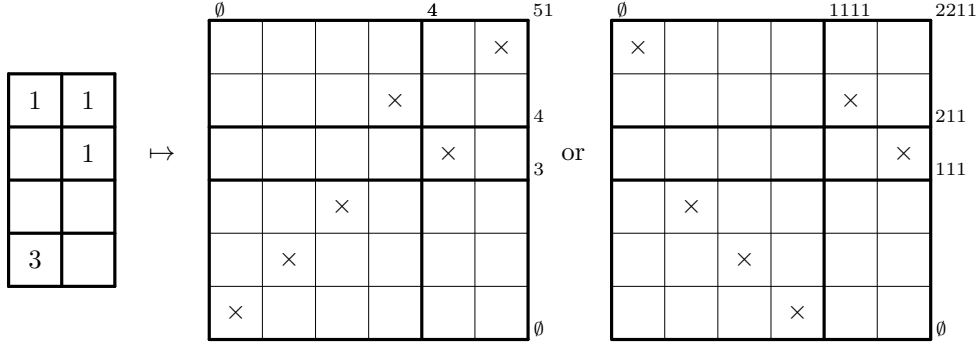


FIGURE 4. standardisation of an arbitrary filling using RSK or dual RSK'

formally: we keep only the partitions between ‘compartments’, and partitions are constant across empty rows and columns.

We remark that the partitions  $\lambda^{i-1}$  and  $\lambda^i$ , as well as  $\mu^{i-1}$  and  $\mu^i$  differ by a *horizontal strip* each, i.e., by at most one cell in each column. Thus,  $P$  corresponds to a semi-standard Young tableau as follows: we put an entry  $i$  into each cell that is present in  $\lambda^i$  but not in  $\lambda^{i-1}$ . Similarly, also  $Q$  corresponds to a semi-standard Young tableau. In the example of Figure 4 (left diagram), we have

$$(P, Q) = \left( \begin{array}{|c|c|c|c|c|c|} \hline \boxed{3} & & & & & \\ \hline \boxed{1} & \boxed{1} & \boxed{1} & \boxed{2} & \boxed{3} & \\ \hline \end{array}, \begin{array}{|c|c|c|c|c|c|} \hline \boxed{2} & & & & & \\ \hline \boxed{1} & \boxed{1} & \boxed{1} & \boxed{1} & \boxed{2} & \\ \hline \end{array} \right).$$

It is well known that  $(P, Q)$  coincides with the result of applying the usual ‘Robinson-Schensted-Knuth’, short RSK correspondence, to  $\pi$ .

We stress that the partitions in  $\bar{P}$  and  $\bar{Q}$  can be reconstructed from those in  $P$  and  $Q$  alone, given the knowledge that the non-zero entries of the filling within compartments should be arranged in north-east chains. In fact, the local rules F1 to F4 and B1 to B4 can be adapted to work *directly* on the original diagrams, bypassing the standardisation process entirely. The details can be found in Christian Krattenthaler’s article [15], Section 4. For convenience, we restate the corresponding variant of Greene’s theorem from [15], Section 4:

**Theorem 3.3.** *Suppose that a corner  $c$  of a growth diagram completed according to the RSK correspondence is labelled by a partition  $\lambda$ . Then, for any integer  $k$ , the maximal cardinality of a union of  $k$  pairwise disjoint NE-chains situated in the rectangular region to the left and below of  $c$  is equal to  $\lambda_1 + \lambda_2 + \dots + \lambda_k$ .*

*Furthermore, the maximal cardinality of the multiset union of  $k$  se-chains, where any entry  $e$  of the filling appears in at most  $e$  chains, all situated in the rectangular region to the left and below of  $c$ , is equal to  $\lambda'_1 + \lambda'_2 + \dots + \lambda'_k$ .*

**3.3.2. Second Variant: dual RSK'.** There is another obvious possibility to standardise an arbitrary filling. Instead of placing the non-zero entries into the new diagram as north-east chains, we could also arrange them in south-east chains, thus preserving the length of ne- and SE-chains. An example for this transformation is given in Figure 4, the result being the right of the two standardised diagrams.

In this case, the partitions  $\lambda^{i-1}$  and  $\lambda^i$  as well as  $\mu^{i-1}$  and  $\mu^i$  differ by a *vertical strip* each, i.e., by at most one cell in each row. Putting  $i$  into each cell that is present in  $\lambda^i$  but not in  $\lambda^{i-1}$ , we see that  $P$  corresponds to a *transposed* semi-standard Young tableau, similarly for  $Q$ . In the example of Figure 4 (right diagram),

we obtain

$$(P, Q) = \left( \begin{array}{|c|c|} \hline 3 & \\ \hline 1 & \\ \hline 1 & 3 \\ \hline 1 & 2 \\ \hline \end{array}, \begin{array}{|c|c|} \hline 1 & \\ \hline 1 & \\ \hline 1 & 2 \\ \hline 1 & 2 \\ \hline \end{array} \right).$$

What we just described is the growth diagram version of the dual RSK' correspondence, also known as the 'Burge' correspondence.

Greene's theorem now reads as follows:

**Theorem 3.4.** *Suppose that a corner  $c$  of a growth diagram completed according to the dual RSK' correspondence is labelled by a partition  $\lambda$ . Then, for any integer  $k$ , the maximal cardinality of a multiset union of  $k$  ne-chains where any entry  $e$  of the filling appears in at most  $e$  chains, all situated in the rectangular region to the left and below of  $c$  is equal to  $\lambda_1 + \lambda_2 + \dots + \lambda_k$ .*

*Furthermore, the maximal cardinality of the union of  $k$  pairwise disjoint SE-chains situated in the rectangular region to the left and below of  $c$ , is equal to  $\lambda'_1 + \lambda'_2 + \dots + \lambda'_k$ .*

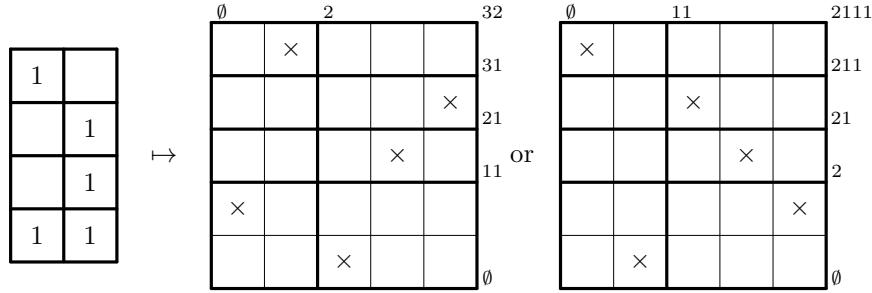


FIGURE 5. standardisation of a 0-1-filling using dual RSK or RSK'

3.3.3. *Third Variant: dual RSK.* If we restrict ourselves to 0-1-fillings, we can also transform multiple non-zero entries of a column of the original diagram into a north-east chain and multiple non-zero entries of a row into a south-east chain. In this case, the lengths of nE- and Se-chains are preserved, as can be seen from the example on the left of Figure 5.

Now  $\lambda^{i-1}$  and  $\lambda^i$  differs by a vertical strip, while  $\mu^{i-1}$  and  $\mu^i$  differs by a horizontal strip. We thus obtain the so-called dual RSK correspondence. In the example of Figure 5 (left diagram), we obtain

$$(P, Q) = \left( \begin{array}{|c|c|c|} \hline 1 & 4 & \\ \hline 1 & 2 & 3 \\ \hline \end{array}, \begin{array}{|c|c|} \hline 2 & 2 \\ \hline 1 & 1 & 2 \\ \hline \end{array} \right),$$

and  $P$  is a transposed semi-standard Young tableau, while  $Q$  is a semi-standard Young tableau.

Again we note the corresponding variation of Greene's theorem:

**Theorem 3.5.** *Suppose that a corner  $c$  of a growth diagram completed according to the dual RSK correspondence is labelled by a partition  $\lambda$ . Then, for any integer  $k$ , the maximal cardinality of a union of  $k$  pairwise disjoint nE-chains situated in the rectangular region to the left and below of  $c$  is equal to  $\lambda_1 + \lambda_2 + \dots + \lambda_k$ .*

*Furthermore, the maximal cardinality of the union of  $k$  pairwise disjoint Se-chains situated in the rectangular region to the left and below of  $c$ , is equal to  $\lambda'_1 + \lambda'_2 + \dots + \lambda'_k$ .*

3.3.4. *Fourth Variant: RSK'*. As a last possibility, again for 0-1-fillings, we can transform multiple non-zero entries of a column of the original diagram into a south-east chain and multiple non-zero entries of a row into a north-east chain, obtaining the ‘Robinson-Schensted-Knuth-prime’ correspondence, short RSK’, which preserves the lengths of Ne- and sE-chains. This is shown on the right of Figure 5.

Here  $\lambda^{i-1}$  and  $\lambda^i$  differs by a horizontal strip, while  $\mu^{i-1}$  and  $\mu^i$  differs by a vertical strip. In the example of Figure 5 (right diagram), we obtain

$$(P, Q) = \left( \begin{array}{|c|c|} \hline 4 & \\ \hline 3 & \\ \hline 2 & \\ \hline 1 & 1 \\ \hline \end{array}, \begin{array}{|c|c|} \hline 2 & \\ \hline 2 & \\ \hline 1 & \\ \hline 1 & 2 \\ \hline \end{array} \right),$$

and  $P$  is a semi-standard Young tableau, while  $Q$  is a transposed semi-standard Young tableau.

Thus, the last variation of Greene’s theorem is:

**Theorem 3.6.** *Suppose that a corner  $c$  of a growth diagram completed according to the RSK’ correspondence is labelled by a partition  $\lambda$ . Then, for any integer  $k$ , the maximal cardinality of a union of  $k$  pairwise disjoint Ne-chains situated in the rectangular region to the left and below of  $c$  is equal to  $\lambda_1 + \lambda_2 + \dots + \lambda_k$ .*

*Furthermore, the maximal cardinality of the union of  $k$  pairwise disjoint sE-chains situated in the rectangular region to the left and below of  $c$ , is equal to  $\lambda'_1 + \lambda'_2 + \dots + \lambda'_k$ .*

#### 4. JEU DE TAQUIN AND PROMOTION

Our second tool is *jeu de taquin*, introduced by Marcel Schützenberger, an algorithm that ‘rectifies’ a skew semi-standard Young tableau. For our purposes it is not necessary to introduce skew tableaux, and what we call *jeu de taquin* is sometimes referred to as the  $\Delta$ -operator, eg. in Bruce Sagan’s book [20]. Because of its simplicity, we begin with the description for partial tableaux.

Given a partial Young tableau  $P$ , we define  $jdt(P)$  as the result of the following algorithm:

- (1) subtract one from all the entries in the tableau.
- (2) if present, replace the cell containing 0 by an empty cell. Otherwise stop.  
In the following, we will move the empty cell to the top right border of the tableau, given French notation.
- (3) if there is no cell to the right and no cell above the empty cell, remove the empty cell and stop.
- (4) consider the cells above and to the right of the cell without entry, and exchange the cell with the smaller entry and the empty cell. Go to Step 3.

This variation of *jeu de taquin* can be conveniently described with ‘growth diagrams’ – of a different kind than those introduced in Section 3.1 – as follows: consider a weakly increasing sequence of partitions  $P = (\emptyset = \lambda^0, \lambda^1, \dots, \lambda^n)$  where  $\lambda^{i-1}$  and  $\lambda^i$  differ in size by at most one for  $i \in \{1, 2, \dots, n\}$ . (Note that such a sequence corresponds to a partial Young tableau as described in Section 3.2.) To  $P$  we associate  $jdt(P) = (\emptyset = \mu^0, \mu^1, \dots, \mu^{n-1})$ , with the same property as follows:

If  $\lambda^1 = \emptyset$ , we set  $\mu^i = \lambda^{i+1}$  for  $i < n$ . Otherwise, let  $\mu^0 = \emptyset$ . Suppose that we have already constructed  $\mu^{i-1}$  for some  $i < n$ . Then we distinguish three cases: if  $\lambda^{i+1} = \lambda^i$ , then we set  $\mu^i = \mu^{i-1}$ .

If  $\nu$  is the only partition that contains  $\mu^{i-1}$  and is contained in  $\lambda^{i+1}$ , we set  $\mu^i = \nu$ . Otherwise, there will be exactly one such partition different from  $\lambda^i$ , and we set  $\mu^i$  equal to this partition.

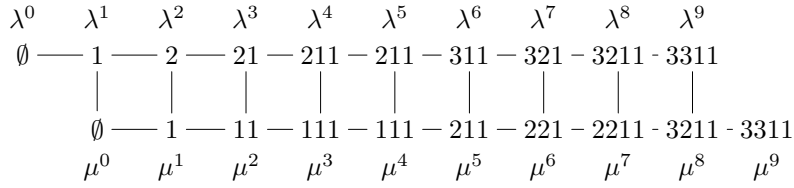


FIGURE 6. jeu de taquin and promotion

The following variation of *jeu de taquin* is usually called *promotion*:  $\overline{jdt}(P)$  is the sequence of partitions obtained by appending the final partition of  $P$  to  $jdt(P)$ . An example for this algorithm can be found in Figure 6. Note that promotion is invertible.

**4.1. Jeu de Taquin and Promotion for Semi-Standard Young Tableaux.**

The description of *jeu de taquin* is slightly more complicated for semi-standard Young tableaux, especially in terms of local rules, which are not as well known as in the standard case.

Given a semi-standard Young tableau  $P$ , we define  $jdt(P)$  as the result of the following algorithm:

- (1) subtract one from all the entries in the tableau.
- (2) if present, replace the cells containing 0 by empty cells. Otherwise stop.
- (3) pick the rightmost empty cell.
- (4) if there is no cell to the right and no cell above the empty cell, remove the empty cell. Go to Step 3.
- (5) consider the cells above and to the right of the empty cell. If there is only one such cell, exchange it with the empty cell. If both cells contain the same entry, exchange the upper cell with the empty cell. Otherwise exchange the cell with the smaller entry and the empty cell. Go to Step 4.

We remark that the conditions in Step 5 are conceived in such a way that the result is again a semi-standard Young tableau.

We now reproduce the description of *jeu de taquin* with local rules, as given by Tom Roby, Frank Sottile, Jeff Stroomer and Julian West in [19, Theorem 4.2]. Given a weakly increasing sequence of partitions  $P = (\emptyset = \lambda^0, \lambda^1, \dots, \lambda^n)$  where  $\lambda^{i-1}$  and  $\lambda^i$  differ by a horizontal strip, we associate  $jdt(P) = (\emptyset = \mu^0, \mu^1, \dots, \mu^{n-1})$ , with the same property as follows:

If  $\lambda^1 = \emptyset$ , we set  $\mu^i = \lambda^{i+1}$  for  $i < n$ . Otherwise, let  $\mu^0 = \emptyset$ . Suppose that we have already constructed  $\mu^{i-1}$  for some  $i < n$ . If  $\lambda^{i+1} = \lambda^i$ , set  $\mu^i = \mu^{i-1}$ .

Otherwise colour the cells of  $\lambda^{i+1}$  that are not in  $\lambda^i$  green, and the cells that are in  $\lambda^i$  but not in  $\mu^{i-1}$  red. Since  $\lambda^{i+1}$  and  $\lambda^i$  differ by a horizontal strip, and so do  $\lambda^i$  and  $\mu^{i-1}$ , a column contains at most two coloured cells, and if so, they have different colours. We now produce a new colouring with the same property as follows: in each column that contains cells of both colours, exchange the two cells. Then, rearrange the coloured cells in each row such that all red cells are to the right of the green cells.  $\mu^i$  is then the shape obtained by removing the red cells.

As in the standard case,  $\overline{jdt}(P)$  is the sequence of partitions obtained by appending the final partition of  $P$  to  $jdt(P)$ . For convenience, if  $P$  is a transposed semi-standard Young tableaux, we define  $jdt(P)$  as  $jdt(P^t)^t$  and  $\overline{jdt}(P)$  as  $\overline{jdt}(P^t)^t$ .

**4.2. Jeu de Taquin and Promotion for Fillings.** The main idea of this article is to define operations analogous to  $\overline{jdt}$  for rectangular fillings:

**Definition 4.1.** Let  $\pi$  be a filling of a rectangular polyomino, and let  $(P, Q)$  be the corresponding pair of sequences of partitions. Then  $\overline{j}(\pi)$  is the filling corresponding to  $(\overline{jdt}(P), Q)$ . An example of this transformation applied to a standard filling can be found in Figure 3.

Note that, like  $\overline{jdt}$ , this transformation is invertible. Furthermore, it is important to keep in mind that in the case of non-standard fillings the result of  $\overline{j}$  depends on the variation of the Robinson-Schensted-Knuth correspondence employed.

In general the transformation  $\overline{j}$  does not preserve the number of entries of a given size, if we are using one of the first two methods of Section 3.3 to standardise the diagram. For example, using Burge's method,  $\begin{array}{|c|c|} \hline 1 & 1 \\ \hline & 1 \\ \hline \end{array}$  is mapped to  $\begin{array}{|c|c|} \hline 2 & \\ \hline & 1 \\ \hline \end{array}$ . However, there is a notable exception to this failure: 0-1-fillings where each non-zero entry is the only one in its row or column are mapped to 0-1-fillings with the same restriction. Of course, if we use the method corresponding to RSK' or dual RSK, this is also the case.

The following proposition is a consequence of [21, Corollary A.1.2.6], as pointed out in the proof of [21, A.1.2.10]:

**Proposition 4.2.** Let  $\pi$  be a filling of a rectangular polyomino, and let  $Q$  be the sequence of partitions in the top row of the associated growth diagram. Let  $R$  be the sequence of partitions in the top row of the growth diagram corresponding to  $\pi$  with the first column deleted. Then  $R = jdt(Q)$ .

This proposition might suggest the following alternative description of  $\overline{j}(\pi)$ : first standardise  $\pi$  as in Section 3.3. Suppose that the first column of  $\pi$  has column-sum  $k$ , then apply  $\overline{j}$  as defined for partial fillings  $k$  times. Finally shrink back the diagram again.

However, it turns out that standardisation does not commute with promotion, and therefore this idea will not work. In particular, the non-zero entries in the last  $k$  columns will in general not form a north-east or south-east chain as they should

in the standardisation of a filling. For example, consider the filling  $\begin{array}{|c|c|c|} \hline & 1 & \\ \hline 1 & & 1 \\ \hline 2 & 1 & \\ \hline \end{array}$ , and

suppose we are interested in North-East chains, i.e., we want to use RSK. Then, the standardised filling is as on the left of Figure 7. Applying  $\overline{j}$  three times gives the filling in the middle of Figure 7, which clearly differs from the standardisation

of  $\overline{j}(\pi) = \begin{array}{|c|c|c|} \hline 1 & & \\ \hline 1 & & 1 \\ \hline & 1 & 2 \\ \hline \end{array}$ , which is depicted on the right.

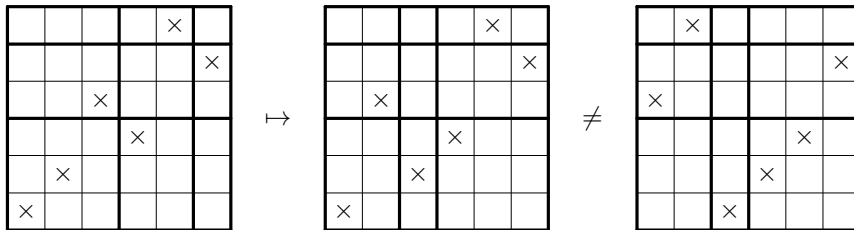


FIGURE 7. standardisation does not commute with promotion

In Lemma 4.6 we will see that a slight weakening of such a commutation property is true.

**Definition 4.3.** Two (arbitrary) fillings of a rectangular polyomino are *Knuth equivalent* if the corresponding partitions labelling the corners along the right border are the same. They are *dual Knuth equivalent* if the corresponding partitions labelling the corners along the upper border are the same.

Our proof of Jakob Jonsson’s conjecture relies heavily on the following two propositions, that show in which situation Knuth equivalence is preserved.

**Proposition 4.4.** *Suppose that the fillings  $\boxed{\alpha}$  and  $\boxed{\alpha'}$  are Knuth equivalent, and so are  $\boxed{\beta}$  and  $\boxed{\beta'}$ . Then also  $\boxed{\alpha|\beta}$  and  $\boxed{\alpha'|\beta'}$  are Knuth equivalent.*

*Similarly, if  $\boxed{\alpha}$  and  $\boxed{\alpha'}$  are dual Knuth equivalent, and so are  $\boxed{\beta}$  and  $\boxed{\beta'}$ , then also  $\boxed{\beta|\alpha}$  and  $\boxed{\beta'|\alpha'}$  are dual Knuth equivalent.*

*Proof.* This is just saying that the plactic monoid is indeed a monoid. □

**Proposition 4.5.** *Consider the filling  $\pi'$  defined by columns  $i + 1, i + 2, \dots, i + k$ ,  $i \geq 1$ , of a filling  $\pi$  of a rectangular polyomino. Then  $\pi'$  is dual Knuth equivalent to the filling defined by columns  $i, i + 1, \dots, i + k - 1$  of  $\bar{j}(\pi)$ . Furthermore, the filling defined by rows  $i, i + 1, \dots, i + k$  of  $\pi$  is Knuth equivalent to the filling defined by the same rows of  $\bar{j}(\pi)$ . In particular, row sums are preserved and column sums are cyclically shifted by one.*

*Proof.* Let  $Q$  be the sequence of partitions labelling the upper border of the growth diagram corresponding to  $\pi$ . To obtain the sequence of partitions along the upper border of  $\pi'$ , we have to delete the first  $i$  columns of  $\pi$  and take the first  $k$  partitions labelling the upper border of the growth diagram corresponding to the resulting filling. By Proposition 4.2, this is equivalent to applying  $jdt$  exactly  $i$  times to  $Q$  and keeping only the first  $k$  partitions.

On the other hand the filling defined by columns  $i, i + 1, \dots, i + k - 1$  of  $\bar{j}(\pi)$  is obtained by applying  $\bar{j}$ , then deleting the first  $i - 1$  columns. By the definition of  $\bar{j}$  and Proposition 4.2, the corresponding partitions are again the first  $k$  of  $jdt$  applied  $i$  times to  $Q$ .

To prove the second statement, note first that the sequence of partitions  $P$  along the right border of  $\pi$  and  $\bar{j}(\pi)$  are the same by definition. To obtain the sequence of partitions of the filling defined by rows  $i, i + 1, \dots, i + k$  in  $\pi$  or  $\bar{j}(\pi)$ , we can apply  $jdt$  exactly  $i - 1$  times to  $P$  and finally drop all but the first  $k + 1$  partitions. □

With the aid of the preceding proposition we can also prove the announced commutation property of standardisation and promotion. This will also be needed in the proof of Proposition 4.7.

**Lemma 4.6.** *Let  $\pi$  be an arbitrary filling of a rectangle and  $\bar{\pi}$  the following partial standardisation of  $\pi$ : each column but the first and each row is replaced by as many columns and rows as it contains non-zero entries, counting multiplicities. The non-zero entries are then placed in chains according to one of the usual standardisation rules. Then we have  $std(\bar{j}(\pi)) = std(\bar{j}(\bar{\pi}))$ .*

For example, if  $\pi$  is 

	1	
1		1
2	1	

, then, using RSK-standardisation,  $\bar{\pi}$  is 

		×	
			×
×			
	×		
×			
×			

.

*Proof.* Since  $\bar{j}$  preserves Knuth equivalence,  $std(\bar{j}(\pi))$  and  $std(\bar{j}(\bar{\pi}))$  are Knuth equivalent. We want to show that the two fillings are also dual Knuth equivalent.

By Proposition 4.5 and Proposition 4.2, all but the last  $m$  partitions along the upper border of  $\text{std}(\bar{j}(\pi))$  and  $\text{std}(\bar{j}(\bar{\pi}))$  are the same, where  $m$  is the sum of the entries in the first column of  $\pi$ .

Furthermore, the but-last partitions of the upper border of  $\bar{j}(\pi)$  and  $\bar{j}(\bar{\pi})$  agree by the definition of  $jdt$ . By the definition of  $\overline{jdt}$ , also the final partitions are equal, which implies the claim.  $\square$

Finally, in Section 6 we will also need the following proposition, for which, unfortunately, we do not have a short proof. It asserts that  $\bar{j}$  preserves locality of modification under a natural condition.

**Proposition 4.7.** *Consider the following two fillings:*

$$\boxed{\alpha|\beta|\delta} \quad \text{and} \quad \boxed{\alpha|\gamma|\delta}$$

*and suppose furthermore that  $\beta$  and  $\gamma$  are Knuth equivalent. Then, applying  $\bar{j}$  to both fillings we obtain*

$$\boxed{\alpha'|\beta'|\delta'} \quad \text{and} \quad \boxed{\alpha'|\gamma'|\delta'}$$

*where  $\alpha'$  has exactly one column less than  $\alpha$  and  $\delta'$  has exactly one more column than  $\delta$ . In this situation,  $\beta'$  and  $\gamma'$  are Knuth equivalent.*

*Similarly, consider*

$$\begin{array}{|c|} \hline \delta \\ \hline \beta \\ \hline \alpha \\ \hline \end{array} \quad \text{and} \quad \begin{array}{|c|} \hline \delta \\ \hline \gamma \\ \hline \alpha \\ \hline \end{array}$$

*and suppose furthermore that  $\beta$  and  $\gamma$  are dual Knuth equivalent. Then, applying  $\bar{j}$  to both fillings we obtain*

$$\begin{array}{|c|} \hline \delta' \\ \hline \beta' \\ \hline \alpha' \\ \hline \end{array} \quad \text{and} \quad \begin{array}{|c|} \hline \delta' \\ \hline \gamma' \\ \hline \alpha' \\ \hline \end{array}$$

*where  $\alpha'$ ,  $\beta'$  and  $\delta'$  have as many rows as  $\alpha$ ,  $\beta$  and  $\delta$  respectively. In this situation,  $\beta'$  and  $\gamma'$  are dual Knuth equivalent.*

*Proof.* The proof is given in the appendix.  $\square$

## 5. INCREASING AND DECREASING SUBSEQUENCES IN FILLINGS OF MOON POLYOMINOES

In this section we will apply the transformation  $\bar{j}$  defined in Definition 4.1 to moon polyominoes, thus proving a conjecture of Jakob Jonsson [12, 13].

Various special cases of this theorem were proved by Jörgen Backelin, Julian West and Guoce Xin [1], Anna de Mier [5], William Chen, Eva Deng, Rosena Du, Richard Stanley and Catherine Yan [3], by Christian Krattenthaler [15], and by Jakob Jonsson and Volkmar Welker [12, 13]. More precisely, in [13] the special case of stack polyominoes is proved, using a very different method. In [1] and [3] the special case of Ferrers shapes is dealt with, under various restrictions on the number of non-zero entries allowed, using completely different methods. In [15] growth diagrams were employed to reprove and generalise the results from [3], and the connection to Jakob Jonsson's conjecture was noticed. In the end, the ideas from [15] led to the proofs given here. For the precise connection between Christian Krattenthaler's theorems and the theorem stated below, see Section 7.

**Theorem 5.1.** *Let  $M$  be a moon polyomino and  $\mathbf{r}$  a vector of non-negative integers. Let  $\mathcal{F}_{01}^{re}(M, l, \mathbf{r})$  be the set of 0-1-fillings of  $M$  having length of the longest north-east chain equal to  $l$  and exactly  $\mathbf{r}_i$  non-zero entries in row  $i$ . Then, for any*

permutation  $\sigma$  of the column indices of  $M$  such that  $\sigma M$  is again a moon polyomino, the cardinalities of  $\mathcal{F}_{01}^{ne}(M, l, \mathbf{r})$  and  $\mathcal{F}_{01}^{ne}(\sigma M, l, \mathbf{r})$  coincide.

In other words, the number of 0-1-fillings of a given moon polyomino with given length of longest north-east chain and given number of non-zero entries in each row does not depend on the ordering of the columns of the polyomino.

Furthermore, the number of 0-1-fillings of a given moon polyomino with a given number of non-zero entries and given length of longest north-east chain depends only on the content of the moon polyomino.

We prove Theorem 5.1 in two steps. First we show that the transformation  $\bar{j}$  from Definition 4.1 can be used to prove a very general result about cardinalities of unions of chains in arbitrary fillings. In a second step we show that this implies the theorem above, albeit in a non-bijective fashion. Thus, the problem of finding a completely bijective proof of Theorem 5.1 remains open. However, it appears that this problem is difficult: Sergi Elizalde [7] solved the first non-trivial case, where the polyomino has triangular shape, the length of the longest north-east chain is two and the number of non-zero entries is maximal. A stronger bijection for the same situation was recently given by Carlos Nicolás [16].

**Definition 5.2.** Let  $M$  be a moon polyomino,  $\mathbf{r}$  and  $\mathbf{c}$  vectors of non-negative integers, and  $\Lambda$  a mapping that associates to every maximal rectangle  $R$  in  $M$  (which is uniquely determined by its height and its width) a partition  $\Lambda(R)$ . Then  $\mathcal{F}^{ne}(M, \Lambda, \mathbf{r}, \mathbf{c})$  is the set of arbitrary fillings of  $M$  with

- sum of entries in row  $i$  equal to  $\mathbf{r}_i$ ,
- sum of entries in column  $i$  equal to  $\mathbf{c}_i$ , and
- for every maximal rectangle  $R$ , the partition  $\Lambda(R) = (\lambda_1^R, \lambda_2^R, \dots)$  is such that the maximum cardinality of a multiset union of  $k$  north-east chains, where any entry  $e$  in  $R$  appears in at most  $e$  chains, equals  $\lambda_1^R + \lambda_2^R + \dots + \lambda_k^R$ .

By the variation of Greene's theorem corresponding to dual RSK', Theorem 3.4, the maximum cardinality of a union of  $k$  South-East chains is then given by the sum of the first  $k$  parts of the transpose of  $\Lambda(R)$ .

Let  $\mathcal{F}^{ne}(M, \Lambda, n)$ , be the corresponding set of fillings with total sum of entries equal to  $n$ , but where no attention to row- or column sums is paid.

We also define the analogous sets of fillings for  $\mathcal{F}^{NE}$ ,  $\mathcal{F}^{nE}$  and  $\mathcal{F}^{Ne}$  by replacing 'north-east' by one of 'North-East', 'north-East', or 'North-east', as appropriate. Again, by the appropriate variation of Greene's theorem, we implicitly place restrictions on the cardinalities of unions of 'south-east', 'South-east', and 'north-East' chains.

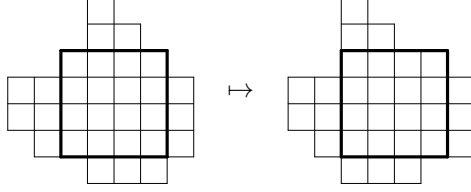
**Theorem 5.3.** Let  $M$  be a moon polyomino and  $\sigma$  a permutation of its columns of the polyomino, such that  $\sigma M$  is again a moon polyomino. Then the sets of maximal rectangles of  $M$  and  $\sigma M$  coincide and there is an explicit bijection between the fillings in  $\mathcal{F}^{ne}(M, \Lambda, \mathbf{r}, \mathbf{c})$  and  $\mathcal{F}^{ne}(\sigma M, \Lambda, \mathbf{r}, \sigma \mathbf{c})$ , for any value of  $\Lambda$ ,  $\mathbf{r}$  and  $\mathbf{c}$ , where  $\sigma \mathbf{c}$  is the vector obtained by permuting the entries of  $\mathbf{c}$  according to  $\sigma$ .

Furthermore, the cardinality of  $\mathcal{F}^{ne}(M, \Lambda, n)$  only depends on  $\Lambda$ ,  $n$  and the content of  $M$ , but not  $M$  itself.

Analogous statements hold for  $\mathcal{F}^{NE}$ ,  $\mathcal{F}^{nE}$  and  $\mathcal{F}^{Ne}$ .

*Proof.* We first show that reordering the columns of the moon polyomino such that the result is again a moon polyomino does not change the number of fillings in question. It suffices to show this in the following special case: let  $c_1$  be the  $x$ -coordinate of any column of the moon polyomino that is contained in one of the columns to its right, i.e., a column to the left of the tallest column. Consider the largest rectangle completely contained in the moon polyomino that has the same

height as the column at  $c_1$ . Then we have to show that moving the first column of this rectangle to the other end of the rectangle, say just after the column with  $x$ -coordinate  $c_2$  does not change the number of fillings with the constraints imposed. For example, we could modify a moon polyomino as follows:



In other words, we cyclically shift the columns between  $c_1$  and  $c_2$ .

We now apply the following bijective transformation to the filling of the moon polyomino: all the entries outside of the rectangle stay as they are, whereas we apply  $\bar{j}$  to the entries within the rectangle. We have to show that this transformation preserves all the statistics mentioned in the statement of the theorem.

By the last statement of Proposition 4.5, the sum of the entries in each row remains the same, and the column sums are cyclically shifted, exactly as the columns themselves.

We first show that there is a one-to-one correspondence between maximal rectangles in the two polyominoes. Consider any maximal rectangle in the original polyomino with first column at  $d_1$  and last column at  $d_2$ . Then, because the polyomino is intersection-free, we have either  $d_1 \leq c_1 < c_2 \leq d_2$  or  $c_1 < d_1 \leq d_2 \leq c_2$ .

In the first case, the corresponding rectangle, of the same height and width, in the new polyomino also consists of the columns between  $d_1$  and  $d_2$ . In the second case, because of the cyclic shift, it consists of the columns from  $d_1 - 1$  up to  $d_2 - 1$ .

It remains to show that the fillings of corresponding maximal rectangles have for every  $k$  the same maximum cardinality of a union of  $k$  north-east chains. (Recall that  $\bar{j}$  depends on the variation of the Robinson-Schensted-Knuth correspondence employed, that is, this determines whether we are going to preserve maximal cardinalities of unions of north-east, North-East, north-East or North-east-chains. For brevity, we assume that we want to preserve north-east chains here.)

We argue that, more precisely, if  $d_1 \leq c_1 < c_2 \leq d_2$ , the fillings of the two rectangles are Knuth equivalent, whereas, if  $c_1 < d_1 \leq d_2 \leq c_2$  they are dual Knuth equivalent.

To see this, we have to combine Propositions 4.5 and 4.4: suppose first that  $d_1 \leq c_1 < c_2 \leq d_2$ , and that the original filling of the rectangle is  $\begin{bmatrix} \alpha & \beta & \delta \end{bmatrix}$ , such that  $\beta$  is the restriction of the filling between  $c_1$  and  $c_2$  to the appropriate rows. The transformation we used leaves entries outside the maximal rectangle between  $c_1$  and  $c_2$  unmodified, therefore, the filling of the rectangle in the transformed polyomino is  $\begin{bmatrix} \alpha & \beta' & \delta \end{bmatrix}$ . By Proposition 4.5,  $\beta$  and  $\beta'$  are Knuth equivalent, and therefore, by Proposition 4.4,  $\begin{bmatrix} \alpha & \beta & \delta \end{bmatrix}$  and  $\begin{bmatrix} \alpha & \beta' & \delta \end{bmatrix}$  must be Knuth equivalent, too.

In case  $c_1 < d_1 \leq d_2 \leq c_2$ , suppose that the original filling of the maximal rectangle between columns  $d_1$  and  $d_2$  is  $\begin{bmatrix} \delta \\ \beta \\ \alpha \end{bmatrix}$ , where  $\beta$  is the restriction of the maximal

rectangle between  $c_1$  and  $c_2$  to the columns between  $d_1$  and  $d_2$ . Similarly, let  $\begin{bmatrix} \delta \\ \beta' \\ \alpha \end{bmatrix}$  be the filling of the rectangle in the transformed polyomino. By Proposition 4.5,  $\beta$  and  $\beta'$  are dual Knuth equivalent, and therefore, by Proposition 4.4,  $\begin{bmatrix} \delta \\ \beta \\ \alpha \end{bmatrix}$  and  $\begin{bmatrix} \delta \\ \beta' \\ \alpha \end{bmatrix}$  must be dual Knuth equivalent, too.

To prove the second claim, let  $F$  be the Ferrers shape with column heights given by the content of  $M$ . We exhibit a bijection between fillings in  $\mathcal{F}^{ne}(M, \Lambda, n)$  and  $\mathcal{F}^{ne}(F, \Lambda, n)$  for any value of  $\Lambda$  and  $n$ .

To do so, we first sort the columns according to their height, using the transformation just described, in decreasing order. This is possible, because moon polyominoes are intersection-free. We then reflect the polyomino about the line  $x = y$ , and obtain a stack polyomino. Note that reflecting the polyomino preserves ne-chains. Once more we sort the columns of the resulting stack polyomino according to height, preserving maximal cardinalities of unions of ne-chains. Finally, we reflect the result again about the line  $x = y$  and obtain a filling of a Ferrers shape with the same content as the original moon polyomino.

The proof showing that  $\mathcal{F}^{NE}(M, \Lambda, n)$  and  $\mathcal{F}^{NE}(F, \Lambda, n)$  have the same cardinality is identical to the foregoing, however, for the other two cases we have to point out a subtlety: suppose that we want to preserve maximal cardinalities of unions of nE-chains. As before, we first sort the columns according to their height transforming the filling such that nE-chains are preserved. Then we reflect the polyomino about the line  $x = y$ . However, reflection transforms nE-chains into Ne-chains. Therefore, we have to use the variant of  $\bar{j}$  that preserves Ne chains to transform the stack-polyomino into a Ferrers shape. Upon reflecting again, we obtain the desired result.  $\square$

The proof above does not imply Theorem 5.1: as we observed before, the transformation  $\bar{j}$  does not preserve the number of entries of a given size. However, a simple inductive argument allows us to reduce it to the statement about arbitrary fillings of Theorem 5.3:

*Proof of Theorem 5.1.* Let  $\mathcal{F}(M, l, \mathbf{r}, \mathbf{m})$  be the set of arbitrary fillings of  $M$  having length of the longest north-east chain equal to  $l$ , sum of entries in row  $i$  equal to  $\mathbf{r}_i$  and  $\mathbf{m}_i$  non-zero entries in row  $i$ . Note that  $\mathcal{F}(M, l, \mathbf{r}, \mathbf{r})$  is just the set of 0-1-fillings  $\mathcal{F}_{01}^{ne}(M, l, \mathbf{r})$ .

We will show by induction on the total number  $|\mathbf{m}|$  of non-zero entries in the fillings that  $|\mathcal{F}(M, l, \mathbf{r}, \mathbf{m})| = |\mathcal{F}(\sigma M, l, \mathbf{r}, \mathbf{m})|$ , for any permutation  $\sigma$  such that  $\sigma M$  is again a moon polyomino.

When  $|\mathbf{m}| = 1$ , there is only one non-zero entry in the filling, and therefore  $\mathcal{F}(M, l, \mathbf{r}, \mathbf{m}) = \mathcal{F}(\sigma M, l, \mathbf{r}, \mathbf{m})$ . Suppose now that  $|\mathbf{m}| > 1$ . By induction, we have that

$$\sum_{|\mathbf{k}| < |\mathbf{m}|} |\mathcal{F}(M, l, \mathbf{m}, \mathbf{k})| = \sum_{|\mathbf{k}| < |\mathbf{m}|} |\mathcal{F}(\sigma M, l, \mathbf{m}, \mathbf{k})|.$$

Furthermore, by Theorem 5.3, we know that the number of arbitrary fillings of  $M$  and  $\sigma M$  with sum of entries in row  $i$  equal to  $\mathbf{m}_i$  coincide:

$$\sum_{|\mathbf{k}| \leq |\mathbf{m}|} |\mathcal{F}(M, l, \mathbf{m}, \mathbf{k})| = \sum_{|\mathbf{k}| \leq |\mathbf{m}|} |\mathcal{F}(\sigma M, l, \mathbf{m}, \mathbf{k})|.$$

Therefore we must have equality of  $|\mathcal{F}(M, l, \mathbf{m}, \mathbf{m})|$  and  $|\mathcal{F}(\sigma M, l, \mathbf{m}, \mathbf{m})|$ , i.e., the number of 0-1-fillings of the two polyominoes coincide.

To complete the induction step, it remains to show that

$$|\mathcal{F}(M, l, \mathbf{r}, \mathbf{m})| = |\mathcal{F}(\sigma M, l, \mathbf{r}, \mathbf{m})|$$

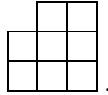
for arbitrary  $\mathbf{r}$ . To do so, let  $\mathbf{k}_i$  be a composition of  $\mathbf{r}_i$  with  $\mathbf{m}_i$  parts. Replacing the ones in a filling in  $\mathcal{F}(M, l, \mathbf{m}, \mathbf{m})$  – which is a 0-1-filling – with the parts of the composition, we obtain a filling in  $\mathcal{F}(M, l, \mathbf{r}, \mathbf{m})$ . Moreover, every filling in  $\mathcal{F}(M, l, \mathbf{r}, \mathbf{m})$  is obtained in such a way. Since the number of ones in members of  $\mathcal{F}(M, l, \mathbf{m}, \mathbf{m})$  and  $\mathcal{F}(\sigma M, l, \mathbf{m}, \mathbf{m})$  coincide in every row, we are done.

The proof of the second claim, namely that the number of 0-1-fillings of a given moon polyomino with a given number of non-zero entries and given length of longest north-east chain depends only on the content of the polyomino, is quite similar. Let  $\mathcal{F}(M, l, n, m)$  be the set of arbitrary fillings of  $M$  having length of the longest north-east chain equal to  $l$ , sum of entries equal to  $n$  and  $m$  non-zero entries. We show by induction on  $m$  that  $|\mathcal{F}(M, l, n, m)| = |\mathcal{F}(F, l, n, m)|$ , where  $F$  is the Ferrers shape with column heights given by the content of  $M$ . The only difference to the foregoing is, that we now have to invoke the second statement of Theorem 5.3, saying that the the number of arbitrary fillings of  $M$  only depends on the contents of  $M$ .  $\square$

We conclude this section with counterexamples to a few seemingly natural generalisations of Theorem 5.1. First, note that we cannot restrict the length of the longest NE-chain (or, if preferred: SE-chain) instead, not even for stack polyominoes. Indeed, consider the following filling of a stack polyomino:

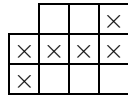


Its longest NE-chain has length 3. However, there is no such filling with seven non-zero entries of the stack polyomino

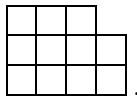


In particular, this also implies that one cannot hope to be able to preserve both the length of the longest ne- and SE-chains.

Similarly, we cannot preserve simultaneously the length of the longest ne- and se-chain. The following example shows that this is impossible if we additionally insist on preserving the number of non-zero entries in each row:



is a filling with longest north-east chain having length two, and longest south-east chain having length one. On the other hand, there is no such filling of the polyomino



Anna de Mier [5] found a counterexample also for the general case.

Finally, we remark that it is not possible to preserve both row and column sums analogous to the statement in Theorem 5.3. Consider for example the filling



There is only one filling with row sums 3, 1, 1 and column sums 1, 3, 1 of the permuted polyomino, namely



but this has a north-east chain of length two.

6. A COMMUTATION PROPERTY

In this section we would like to prove another beautiful feature of the transformation  $\bar{j}$  as applied in the proof of Theorem 5.3:

**Theorem 6.1.** *Applications of  $\bar{j}$  to different rectangles of a filling of a moon-polyomino  $M$ , such that the first columns of the rectangles are as tall as the respective columns of  $M$ , commute with each other.*

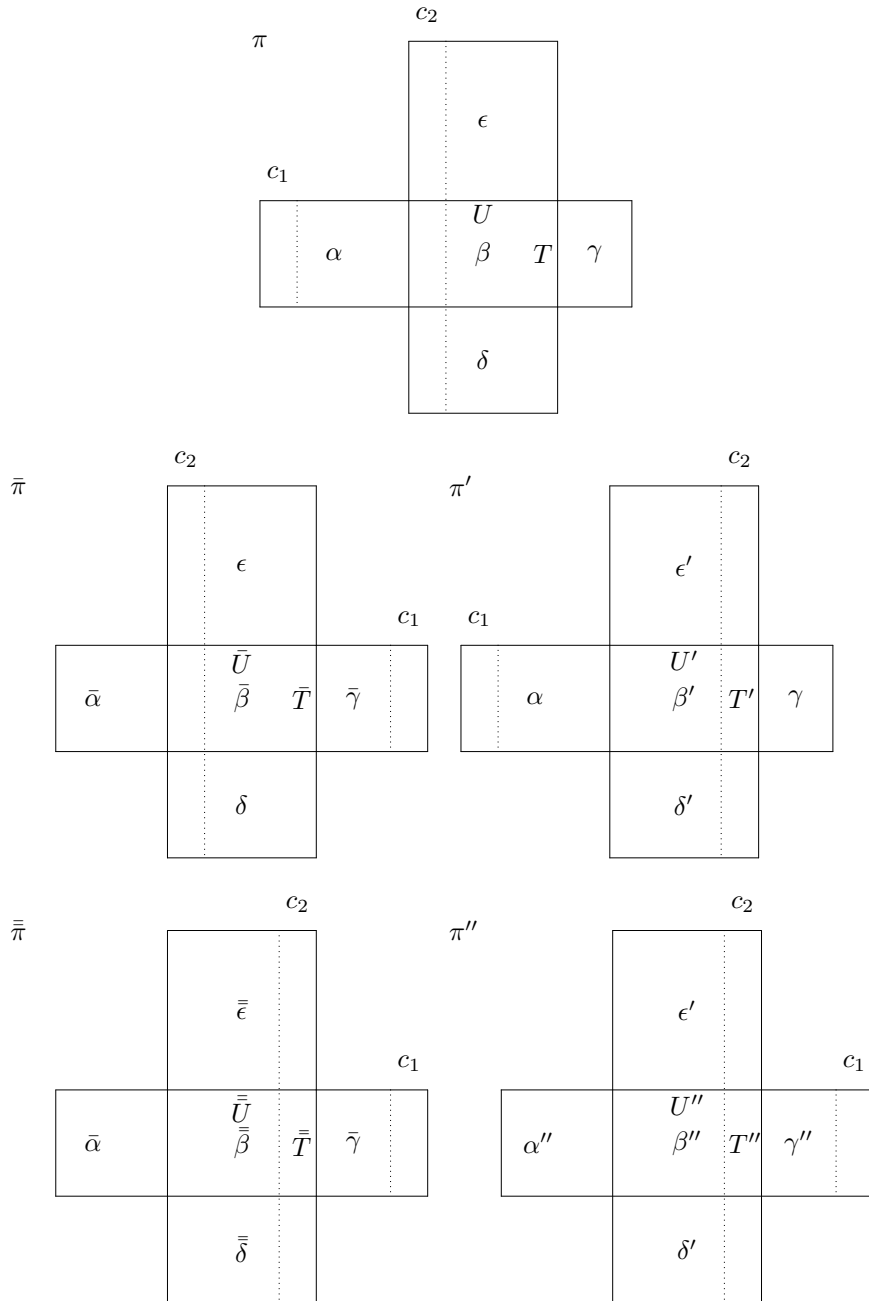


FIGURE 8. applying  $\bar{j}$  successively to  $\Gamma$  and  $\Delta$

*Proof.* Suppose that  $c_1$  and  $c_2$  are respectively the first columns of two maximal rectangles  $\Gamma$  and  $\Delta$  and that we want to move  $c_1$  to the end of the first rectangle, and  $c_2$  towards the end of the second rectangle. Since all entries outside of these two rectangles stay unchanged, we can assume that the moon polyomino consists only of the union of  $\Gamma$  and  $\Delta$ , as schematically depicted at the top of Figure 8. There, we subdivided  $\Gamma$  into three smaller rectangles  $\alpha$ ,  $\beta$  and  $\gamma$  and  $\Delta$  into  $\delta$ ,  $\beta$  and  $\epsilon$ .

In the following we will have to consider several growth diagrams simultaneously. In particular, we consider the growth diagram corresponding to  $\beta$  and will label its top and right border with sequences of partitions  $U$  and  $T$ .

On the left hand side of Figure 8 we see what happens to the original filling

when we apply  $\bar{j}$  first to the rectangle  $\Gamma = \begin{array}{|c|c|c|} \hline \alpha & \beta & \gamma \\ \hline \end{array}$ , to obtain  $\bar{\pi}$ , and then to  $\begin{array}{|c|} \hline \epsilon \\ \beta \\ \delta \\ \hline \end{array}$

to obtain  $\bar{\bar{\pi}}$ . On the right hand side the result  $\pi'$  of applying  $\bar{j}$  first to the rectangle

$\Delta = \begin{array}{|c|} \hline \epsilon \\ \beta \\ \delta \\ \hline \end{array}$  and then the result  $\pi''$  of applying  $\bar{j}$  to  $\begin{array}{|c|c|c|} \hline \alpha & \beta' & \gamma \\ \hline \end{array}$  is shown. We have to

prove that the fillings  $\bar{\bar{\pi}}$  and  $\pi''$  at the bottom of Figure 8 are the same.

We first observe that  $\begin{array}{|c|} \hline \beta \\ \hline \end{array}$  and  $\begin{array}{|c|} \hline \beta' \\ \hline \end{array}$  are Knuth equivalent. This follows by applying

the second part of Proposition 4.5 to the rows corresponding to  $\beta$  in  $\begin{array}{|c|} \hline \epsilon \\ \beta \\ \delta \\ \hline \end{array}$ . Thus we

can apply the first part of Proposition 4.7 to  $\begin{array}{|c|c|c|} \hline \alpha & \beta & \gamma \\ \hline \end{array}$  and  $\begin{array}{|c|c|c|} \hline \alpha & \beta' & \gamma \\ \hline \end{array}$  and obtain that  $\bar{\alpha} = \alpha''$ ,  $\bar{\gamma} = \gamma''$  and  $\bar{T} = T''$ . Again by the second part of Proposition 4.5,

applied to the rows corresponding to  $\bar{\beta}$  in  $\begin{array}{|c|} \hline \epsilon \\ \bar{\beta} \\ \delta \\ \hline \end{array}$  we have that  $\bar{T} = \bar{\bar{T}}$ .

Very similarly, applying the first part of Proposition 4.5, we observe that  $\begin{array}{|c|} \hline \beta \\ \hline \end{array}$  and  $\begin{array}{|c|} \hline \bar{\beta} \\ \hline \end{array}$  are dual Knuth equivalent. Thus, the second part of Proposition 4.7 applied

to  $\begin{array}{|c|} \hline \epsilon \\ \beta \\ \delta \\ \hline \end{array}$  and  $\begin{array}{|c|} \hline \epsilon \\ \bar{\beta} \\ \delta \\ \hline \end{array}$ , shows that  $\bar{\delta} = \delta'$ ,  $\bar{\epsilon} = \epsilon'$  and  $\bar{U} = U'$ . By the first part of

Proposition 4.5 we have  $U' = U''$ .

Finally,  $\bar{\beta} = \beta''$  follows from  $\bar{\bar{T}} = T''$  and  $\bar{U} = U''$ .  $\square$

## 7. EVACUATION AND PROMOTION FOR STACK POLYOMINOES

In this section we relate our bijection to evacuation, and thereby to the construction employed by Christian Krattenthaler [15] to prove Theorem 5.1 and Theorem 5.3 for the special case of Ferrers diagrams. Let us first recall the definition of evacuation.

**Definition 7.1.** Given a weakly increasing sequence of partitions  $Q = (\emptyset = \lambda^0, \lambda^1, \dots, \lambda^n)$ , we construct the *evacuated* sequence of partitions  $ev(Q) = (\emptyset = \mu^0, \mu^1, \dots, \mu^n)$  as follows: We set  $\mu^n = \lambda^n$ , and then  $\mu^{n-i}$  equal to the last partition of  $jdt(\dots jdt(Q))$ , where we apply  $jdt$   $i$  times.

Christian Krattenthaler [15] used the following bijection on Ferrers shapes:

**Definition 7.2.** Let  $\pi$  be a filling of a Ferrers shape and  $\Delta$  the associated growth diagram. Let  $e(\Delta)$  be the growth diagram obtained from  $\Delta$  by transposing all the partitions along the top and right border and applying the backward rules B1 to

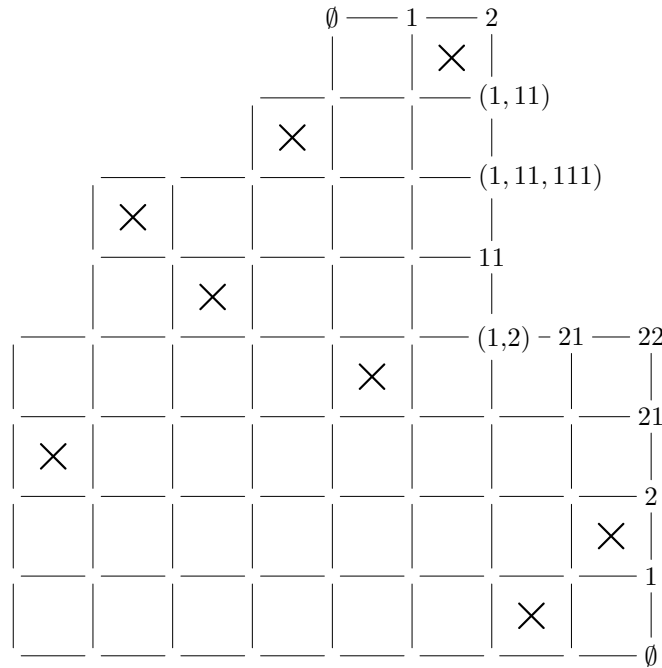


FIGURE 9. a growth diagram for a stack polyomino

B4 to obtain the remaining partitions and the entries of the squares. Let  $e(\pi)$  be the filling associated to  $e(\Delta)$ .

We will show that this bijection is to evacuation what our transformation  $\bar{j}$  is to promotion. To this end we extend the notion of growth diagrams introduced in Section 3 to stack polyominoes.

**7.1. Growth Diagrams for Stack Polyominoes.** Throughout this section, we fix a variant of standardisation.

**Definition 7.3.** Given a filling  $\pi$  of a stack polyomino, we label the top-right corners of the polyomino with *tuples* of partitions to obtain a *growth diagram* as follows:

- if there is no corner directly above the corner  $c$ , or the rows just above and just below it are left-justified, the label consists of a single partition. This partition is computed according to the appropriate variant of Greene’s theorem applied to the filling restricted to the largest rectangle below and to the left of  $c$ .
- Otherwise, suppose that the row above  $c$  is indented to the right by  $m$  columns with respect to the row just below  $c$ : the row just below  $c$  begins in column  $i$ , and the row just below  $c$  in column  $i - m$ . Then the label consists of a tuple of  $m + 1$  partitions: the  $j^{\text{th}}$  partition is computed applying Greene’s theorem to the filling restricted to the largest rectangle below and to the left of  $c$ , beginning in column  $i - j + 1$ .

We say that the sequence of partitions, read beginning at the left-most corner of the top-row, down to the corner at the bottom-right *corresponds* to  $\pi$ .

An example of such a generalised growth diagram is given in Figure 9. It is clear that for Ferrers shapes the construction above coincides with the obvious extension

of growth diagrams as presented in Section 3 and introduced by Sergey Fomin and Tom Roby [8, 18].

Similar to the case of growth diagrams for rectangular shapes we can describe precisely which sequences of partitions labelling the upper-right border actually occur. For partial fillings we have:

**Proposition 7.4.** *Let  $S$  be a stack polyomino. Then there is a bijection between partial fillings of  $S$  and labellings of the top-right corners of  $S$  with tuples of partitions satisfying the following conditions:*

- *the left-most corner in the top row and the corner on the bottom right are labelled with the empty partition.*
- *writing tuples of partitions from left to right, if  $\mu$  is the partition just to the left of  $\lambda$ , then  $\mu$  is obtained from  $\lambda$  by deleting at most one from some part.*
- *if  $\mu$  is the partition just below  $\lambda$ , then  $\mu$  is obtained from  $\lambda$  by deleting at most one from some part.*

*Remark.* To obtain correspondences for arbitrary fillings, we only have to replace ‘deleting at most one from some part’ by ‘deleting a horizontal strip’, or ‘deleting a vertical strip’, according to the chosen variant of standardisation.

*Proof.* For left justified rows we can reconstruct the filling from top to bottom given the partitions along the top and the right corners using the local rules B1 to B4. Thus, the only subtlety is how to deal with successive rows that are not left justified.

Consider the following situation: We are given a tuple  $(\rho_0, \rho_1, \dots, \rho_m)$  of parti-

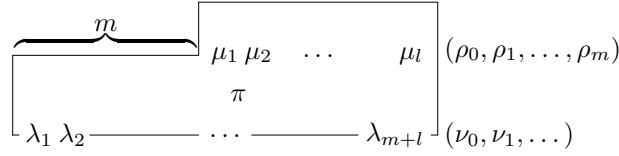


FIGURE 10. reconstructing the partitions labelling the next row

tions labelling the top-right corner of the row, another tuple  $(\nu_0, \nu_1, \dots)$  labelling its bottom-right corner, and partitions  $\emptyset = \mu_0, \mu_1, \dots, \mu_l, \mu_{l+1} = \rho_0$  labelling the corners between the two rows. We would like to determine the filling  $\pi$ , and the sequence of partitions  $\emptyset = \lambda_0, \lambda_1, \dots, \lambda_{m+l}$ .

We want to reconstruct the sequence of partitions  $Q = (\emptyset = \mu'_0, \mu'_1, \dots, \mu'_{m+l})$  such that the last partition of  $Q$  is  $\rho_m$ , the last partition of  $jdt(Q)$  is  $\rho_{m-1}$  and so on. Finally, applying  $jdt$   $m$  times to  $Q$  should yield a sequence of partition ending with  $\rho_0$ . By Proposition 4.2, this is exactly how the partitions labelling the corners of the stack polyomino are computed in Definition 7.3. Given  $Q$  and  $\nu_0$  we can then use the local rules B1 to B4 to compute the filling  $\pi$  and  $\emptyset = \lambda_0, \lambda_1, \dots, \lambda_{m+l}$ .

By considering the growth diagram description of *jeu de taquin* given in Section 4, we see that the preimage of  $jdt$  can indeed be computed, if only one is given the last partition of the preimage. In the first step we compute the preimage of  $(\emptyset = \mu_0, \mu_1, \dots, \mu_{l+1} = \rho_0)$ , assuming as its last partition  $\rho_1$ . We then compute the preimage of this sequence, assuming as its last partition  $\rho_2$ , and so on.  $\square$

**7.2. Evacuation and Promotion.** In this section, we will analyse the effect of reversing the order of the columns of a filling on the sequence of partitions it corresponds to. For rectangular shapes, this is well known:

**Proposition 7.5** (Corollary A 1.2.11 of [21]). *If  $\pi$  corresponds to  $(P, Q)$  then the filling obtained by reversing the order of the columns of  $\pi$  corresponds to  $(P^t, ev(Q)^t)$ .*

To relate our construction to Christian Krattenthaler’s bijection, we will use the following transformation:

**Definition 7.6.** Let  $\pi$  be a filling of a Ferrers shape  $F$ . Let  $ev^t(\pi)$  be the filling of the reversed polyomino obtained by applying  $\overline{j}^{-1}$  to the largest rectangle contained in  $F$  spanning all columns, then  $\overline{j}^{-1}$  to the largest rectangle spanning all columns of the result but the first, and so on.

We can now state and prove the main theorem of this section:

**Theorem 7.7.** *Let  $\pi$  be a filling of a Ferrers shape. Suppose that the sequence of partitions labelling its top-left corners, reading from the left of the top row down to the bottom-right is  $(\emptyset = \lambda_0, \lambda_1, \dots, \lambda_n = \emptyset)$ , and that its top-row consists of  $k$  cells. Let  $\pi^r$  be the filling (of a stack-polyomino) obtained by reflecting  $\pi$  about a vertical line. Then we have:*

- (1) *Let  $(\emptyset = \mu_0, \mu_1, \dots, \mu_n = \emptyset)$  be the sequence of partitions labelling  $\pi^r$ . Then  $(\mu_0^t, \mu_1^t, \dots, \mu_k^t) = ev(\lambda_0, \lambda_1, \dots, \lambda_k)$ , and  $\mu_i^t = \lambda_i$  for  $i \geq k$ .*
- (2) *Let  $(\emptyset = \nu_0, \nu_1, \dots, \nu_n = \emptyset)$  be the sequence of partitions labelling  $ev^t(\pi)$ . Then  $(\nu_0, \nu_1, \dots, \nu_k) = ev(\lambda_0, \lambda_1, \dots, \lambda_k)$ , and  $\nu_i = \lambda_i$  for  $i \geq k$ .*

*Proof.* For rectangular shapes, the first statement is precisely Proposition 7.5. To prove the second statement for rectangular shapes, let the sequence of partitions labelling the right corners of  $\pi$  be  $P$  and let  $Q$  be the sequence of partitions labelling the top corners. Then, by Proposition 4.2, applying  $ev^t$  to  $\pi$  amounts to applying evacuation on  $Q$  and leaving  $P$  unchanged.

To see the first statement for stack polyominoes, consider corresponding partitions in  $\pi$  and its reverse, as in Figure 11. Again, the fillings within the dotted rectangles are just the reversed of each other, and Proposition 7.5 implies  $\mu_i = \lambda_i^t$ .

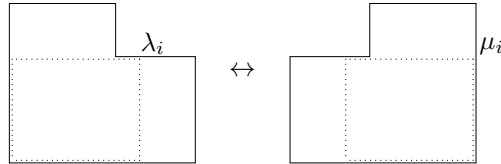


FIGURE 11. corresponding labels of  $\pi$  and its reverse

For the proof of the second statement, suppose that we have already applied  $\overline{j}^{-1}$  several times, and we are now going to apply it to the next block of rectangles of common height, as on the left of Figure 12.

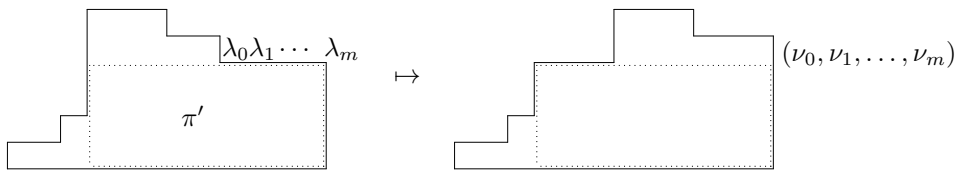


FIGURE 12. applying  $\overline{j}^{-1}$  to a block of rectangles

Since  $\bar{j}^{-1}$  preserves Knuth-equivalence, and we do not modify the filling to the left of the dotted rectangle anymore, Proposition 4.4 implies that the labels below the top row of the dotted rectangle will not be altered. Furthermore, because of Proposition 4.5 and since we do not modify the filling above the dotted rectangle when applying  $\bar{j}^{-1}$  the next  $m$  times, the labels above the top row of the dotted rectangle will also stay the same.

Thus, it remains to show that, with the notation indicated in the picture,  $\lambda_i = \nu_i$ . To this end, consider the filling  $\pi'$  on the left of Figure 12 within the dotted rectangle. We need to compute the effect of applying  $\bar{j}^{-1}$  a total of  $m$  times, first to the full rectangle, then to all but the first column of the result and so on.

The first application of  $\bar{j}^{-1}$  preserves the shape  $\lambda_m$  of the filling. In the following, the first column of the resulting filling is not modified anymore. Since  $\bar{j}^{-1}$  preserves Knuth-equivalence by definition, Proposition 4.4 implies that the shape of the filling of the full rectangle is not modified at all during the remaining  $m - 1$  applications of  $\bar{j}^{-1}$ . Therefore,  $\nu_m = \lambda_m$ .

Furthermore, by Proposition 4.5, the filling obtained from  $\pi'$  by deleting the last column is dual Knuth equivalent to the filling  $\pi''$  obtained from  $\bar{j}^{-1}(\pi')$  by deleting its first column. In particular, the shape of  $\pi''$  is  $\lambda_{m-1}$ , and as before we deduce that  $\nu_{m-1} = \lambda_{m-1}$ . The claim follows by induction.  $\square$

#### APPENDIX A. LOCALITY OF PROMOTION

In this appendix we prove Proposition 4.7. We will first consider only the case of standard fillings, and then deduce the general case using standardisation, using Lemma 4.6.

**Definition A.1.** Two partial fillings differ by a *Knuth relation of the first kind*, if all but three columns coincide, and the remaining three columns are related (schematically) by transforming

$$\begin{array}{|c|c|c|} \hline \times & \times & \\ \hline \times & & \times \\ \hline & \times & \\ \hline \end{array} \text{ into } \begin{array}{|c|c|c|} \hline \times & & \times \\ \hline \times & & \\ \hline & \times & \\ \hline \end{array},$$

or vice versa. They differ by a *Knuth relation of the second kind*, if the remaining three columns are related by transforming

$$\begin{array}{|c|c|} \hline \times & \\ \hline \times & \times \\ \hline \times & \\ \hline \end{array} \text{ into } \begin{array}{|c|c|} \hline \times & \\ \hline \times & \times \\ \hline \times & \times \\ \hline \end{array},$$

or vice versa. The indicated transformations are called *Knuth transformations*.

It is well known that two partial fillings are Knuth equivalent (see Definition 4.3) if and only if they can be transformed one into the other using a sequence of Knuth transformations. The following proposition gives also some information on the sequence of partitions along the upper border of the growth diagram. For its precise statement, we need yet another definition:

**Definition A.2.** A partial filling of a rectangle with three columns is *shape equivalent to a triangle*, if the partition labelling the top right corner of the corresponding growth diagram equals 21.

In terms of tableaux, we say that three consecutive entries  $k - 1$ ,  $k$  and  $k + 1$  of a partial tableau are *shape equivalent to a triangle* if applying  $jdt$   $k - 2$  times to the tableau results in a tableau where the entries 1, 2 and 3 are arranged as

$$\begin{array}{|c|c|} \hline 2 & \\ \hline 1 & 3 \\ \hline \end{array}$$

or

$$\begin{array}{|c|c|} \hline 3 & \\ \hline 1 & 2 \\ \hline \end{array}.$$

**Proposition A.3.** *Two partial fillings differ by a single Knuth relation (of either kind), namely in columns  $k - 1, k$  and  $k + 1$  if and only if the fillings are Knuth equivalent, the sequences of partitions along the upper border of their growth diagrams differ in exactly one partition, namely either between columns  $k - 1$  and  $k$  or  $k$  and  $k + 1$ , and each of the two fillings restricted to these three columns is shape equivalent to a triangle.*

Note that there are Knuth equivalent growth diagrams that differ in exactly one partition along the upper border, but cannot be transformed one into the other by a single Knuth transformation. A small example is given in Figure 13, where we superimposed the two growth diagrams, using crosses for one and circles for the other. We write the partitions belonging to the diagram with circles just above the partitions belonging to the diagram with crosses, wherever the partitions labelling a corner differ. We will keep this notation throughout the appendix.

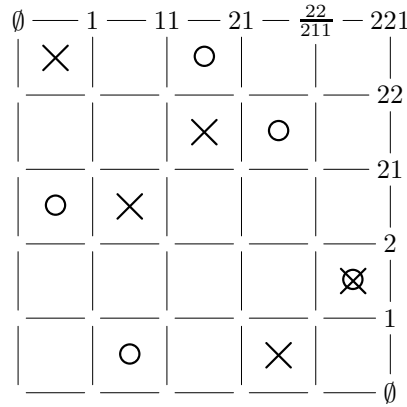


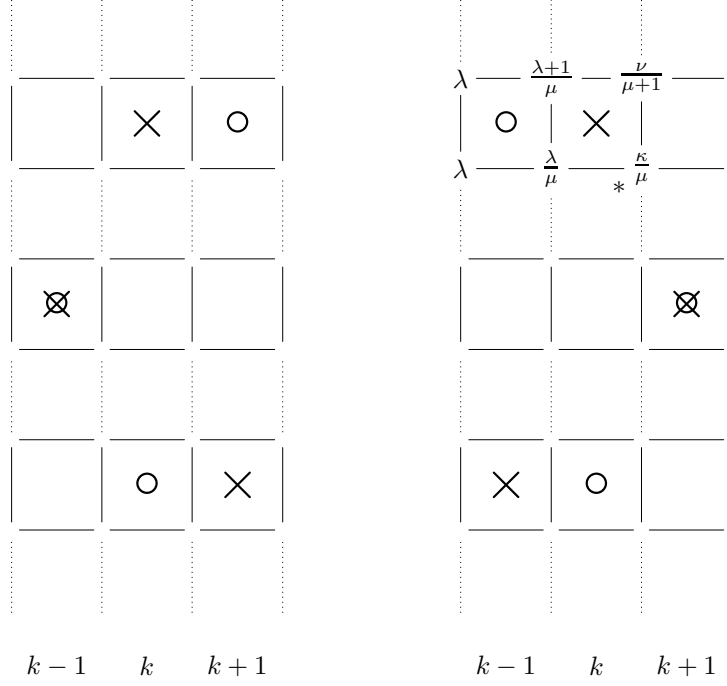
FIGURE 13. Two very different Knuth equivalent fillings, whose growth diagrams differ along the border only in a single partition. The filling with circles is not shape equivalent to a triangle in the last three columns.

*Proof.*  $\Rightarrow$  Suppose that the two growth diagrams differ by a single Knuth relation of the first kind, as shown in Figure 14.a. In this case, all partitions along the upper border up to and including the partition just after column  $k - 1$  must be equal, since, up to this point the fillings are identical. Furthermore, all partitions along the top corner starting with the partition just after column  $k + 1$  must be equal, since the fillings up to that column are Knuth equivalent. We conclude that, in this case, exactly the partitions of the two growth diagrams on the top border just after column  $k$  are different.

It remains to check the case where the two growth diagrams differ by a single Knuth relation of the second kind.

To ease the description, we introduce the following notation: given a partition  $\lambda$ , let  $\lambda + \epsilon_k$  be the result of adding one to the  $k^{\text{th}}$  part of  $\lambda$ . Furthermore, we write  $\lambda + 1$  as shorthand for  $\lambda + \epsilon_1$ . We then have a situation as shown schematically in Figure 14.b.

We first show that, in the situation of Figure 14.b, either  $\mu = \lambda + 1$  or  $\nu = \mu + 1$ . To this end, suppose that  $\mu \neq \lambda + 1$ . Since the fillings in the rectangles below and to the left of  $*$  are equal, with the exception of the position of an empty column,  $\mu = \kappa$ . Applying forward rule F2, it follows that  $\nu = \mu \cup \lambda + 1 = \mu + 1$ .

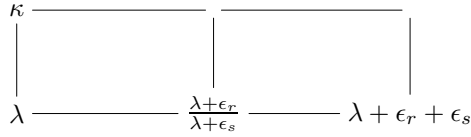


a. Knuth relation of the first kind.    b. Knuth relation of the second kind.

FIGURE 14. Knuth equivalent columns

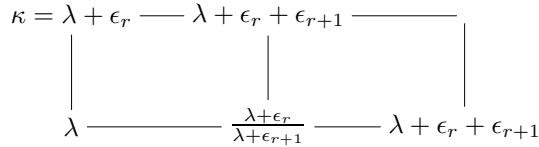
It remains to show that the two growth diagrams differ in exactly one of the two partitions on the upper border. If  $\mu = \lambda + 1$  then, by the forward rules, all partitions on the right side above the circle in column  $k - 1$  are identical, including the partitions on the upper border in this column.

If, however,  $\nu = \mu + 1$ , we have to use an inductive argument to show our claim. Consider the following part of a growth diagram, where both cells are assumed to be empty and  $r \neq s$ :



We will show that no matter what value  $\kappa$  has, there will be again exactly one corner at the top where the partitions of the two growth diagrams differ:

Suppose first, that  $\kappa = \lambda + \epsilon_r$  and  $s = r + 1$ . Applying the forward rules F2 and F3 we obtain



Thus the partitions labelling corners on the right of column  $k - 1$  of the two growth diagrams coincide from hereon, and the claim follows.

If  $\kappa = \lambda + \epsilon_r$ , but  $s \neq r + 1$ , we obtain (remember  $s \neq r$ )

$$\begin{array}{ccccc} \kappa = \lambda + \epsilon_r & \text{---} & \frac{\lambda + \epsilon_r + \epsilon_{r+1}}{\lambda + \epsilon_r + \epsilon_s} & \text{---} & \lambda + \epsilon_r + \epsilon_{r+1} + \epsilon_s \\ | & & | & & | \\ \lambda & \text{---} & \frac{\lambda + \epsilon_r}{\lambda + \epsilon_s} & \text{---} & \lambda + \epsilon_r + \epsilon_s \end{array}$$

Finally, if  $\kappa = \lambda + \epsilon_t$ , with all of  $r, s$  and  $t$  being different, we obtain

$$\begin{array}{ccccc} \kappa = \lambda + \epsilon_t & \text{---} & \frac{\lambda + \epsilon_r + \epsilon_t}{\lambda + \epsilon_s + \epsilon_t} & \text{---} & \lambda + \epsilon_r + \epsilon_s + \epsilon_t \\ | & & | & & | \\ \lambda & \text{---} & \frac{\lambda + \epsilon_r}{\lambda + \epsilon_s} & \text{---} & \lambda + \epsilon_r + \epsilon_s \end{array}$$

In both cases, the situation in the corners of the top row is the same as in the bottom row, and the claim follows.

⊖ We assume now that the sequences of partitions along the upper border of the two Knuth equivalent growth diagrams differ in exactly one partition, namely between columns  $k$  and  $k + 1$ , and that either the three columns  $k - 1, k$  and  $k + 1$  or  $k, k + 1$  and  $k + 2$  are shape equivalent to a triangle.

Distinguishing between several cases, we consider the effect of applying the backward rules B1 to B4 to the partitions labelling the corners of columns  $k - 1, k$  and  $k + 1$ . We will show that, in each row, if not all partitions coincide, either the partitions between columns  $k$  and  $k + 1$  or those between column  $k - 1$  and  $k$  differ, and all others coincide. Working our way from the top of the growth diagrams to the bottom, we can distinguish three stages: in Stage 1, the partitions between columns  $k$  and  $k + 1$  differ. This stage can be followed either by Stage 2 or by Stage 3. In Stage 2, the partitions between columns  $k - 1$  and  $k$  differ and only Stage 3 can follow. Finally, Stage 3 corresponds to those rows, that lie between the entries which are swapped by the Knuth transformation. It is followed by those rows in which all partitions coincide.

Throughout the rest of this proof we will maintain  $r < s$ . To make it easier to keep track of the various situations and make the description more concise, we omit cases which may be obtained by exchanging the two growth diagrams. The backward rules we apply are printed into the corresponding cells wherever appropriate.

- (1) During this stage, the partitions of the two growth diagrams between columns  $k$  and  $k + 1$  differ. The Cases c and f lead directly to Stage 3, whereas Case e leads to Stage 2. All other cases stay within Stage 1.

$$\begin{array}{ccccc} \lambda - \epsilon_r - \epsilon_s & \text{---} & \frac{\lambda - \epsilon_r}{\lambda - \epsilon_s} & \text{---} & \lambda \\ | & & | & & | \\ \lambda - \epsilon_r - \epsilon_s & \text{---} & \frac{\lambda - \epsilon_r}{\lambda - \epsilon_s} & \text{---} & \lambda \\ | & & | & & | \\ \kappa - \epsilon_r - \epsilon_s & \text{---} & \frac{\kappa - \epsilon_r}{\kappa - \epsilon_s} & \text{---} & \kappa \end{array}$$

(a)  $\kappa = \lambda - \epsilon_t$  and  $r, s$  and  $t$  are all different.

$$\begin{array}{ccccc} \lambda - \epsilon_r - \epsilon_s & \text{---} & \frac{\lambda - \epsilon_r}{\lambda - \epsilon_s} & \text{---} & \lambda \\ | & & \text{B2} & & \text{B2} & | \\ \lambda - \epsilon_r - \epsilon_s & \text{---} & \frac{\lambda - \epsilon_r}{\lambda - \epsilon_s} & \text{---} & \lambda \\ | & & | & & | \\ \kappa - \epsilon_r - \epsilon_s & \text{---} & \frac{\kappa - \epsilon_r}{\kappa - \epsilon_s} & \text{---} & \kappa = \lambda - \epsilon_t \end{array}$$

(b)  $\kappa = \lambda - \epsilon_r$  and  $r > 1$ . Since  $r - 1 < r < s$ ,

$$\begin{array}{ccccc} \lambda - \epsilon_r - \epsilon_s & \xrightarrow{\frac{\lambda - \epsilon_r}{\lambda - \epsilon_s}} & & \xrightarrow{\frac{\lambda - \epsilon_r}{\lambda - \epsilon_s}} & \lambda \\ | & \frac{B2}{B1} & | & \frac{B3}{B2} & | \\ \kappa - \epsilon_{r-1} - \epsilon_s & \xrightarrow{\frac{\kappa - \epsilon_{r-1}}{\kappa - \epsilon_s}} & & \xrightarrow{\frac{\kappa - \epsilon_{r-1}}{\kappa - \epsilon_s}} & \kappa = \lambda - \epsilon_r \end{array}$$

(c)  $\kappa = \lambda - \epsilon_r$  and  $r = 1$ .

$$\begin{array}{ccccc} \lambda - \epsilon_1 - \epsilon_s & \xrightarrow{\frac{\lambda - \epsilon_1}{\lambda - \epsilon_s}} & & \xrightarrow{\frac{\lambda - \epsilon_1}{\lambda - \epsilon_s}} & \lambda \\ | & \frac{B2}{B4} & | & \frac{B4}{B2} & | \\ \kappa - \epsilon_s & \xrightarrow{\frac{\kappa}{\kappa - \epsilon_s}} & & \xrightarrow{\frac{\kappa}{\kappa - \epsilon_s}} & \kappa = \lambda - \epsilon_1 \end{array}$$

$\times$                        $\circ$

(d)  $\kappa = \lambda - \epsilon_s$  and  $s \neq r + 1$ .

$$\begin{array}{ccccc} \lambda - \epsilon_r - \epsilon_s & \xrightarrow{\frac{\lambda - \epsilon_r}{\lambda - \epsilon_s}} & & \xrightarrow{\frac{\lambda - \epsilon_r}{\lambda - \epsilon_s}} & \lambda \\ | & \frac{B3}{B2} & | & \frac{B2}{B3} & | \\ \kappa - \epsilon_r - \epsilon_{s-1} & \xrightarrow{\frac{\kappa - \epsilon_r}{\kappa - \epsilon_{s-1}}} & & \xrightarrow{\frac{\kappa - \epsilon_r}{\kappa - \epsilon_{s-1}}} & \kappa = \lambda - \epsilon_s \end{array}$$

Note that, since  $r < s$ , we have automatically  $s > 1$ .

(e)  $\kappa = \lambda - \epsilon_s$  and  $s = r + 1$ ,  $r > 1$ .

In this case we also have to consider the partitions labelling the corners of columns  $k - 1$  and  $k + 2$ .

$$\begin{array}{ccccccc} \lambda - \epsilon_r - \epsilon_{r+1} - \epsilon_t \cdot \lambda - \epsilon_r - \epsilon_{r+1} & \xrightarrow{\frac{\lambda - \epsilon_r}{\lambda - \epsilon_{r+1}}} & & \xrightarrow{\frac{\lambda - \epsilon_r}{\lambda - \epsilon_{r+1}}} & \lambda & \xrightarrow{\quad} & \lambda + \epsilon_u \\ | & \frac{B3}{B3} & | & \frac{B2}{B3} & | & & | \\ \mu & \xrightarrow{\frac{\kappa - 2\epsilon_r}{\kappa - \epsilon_{r-1} - \epsilon_r}} & & \xrightarrow{\frac{\kappa - 2\epsilon_r}{\kappa - \epsilon_{r-1} - \epsilon_r}} & \kappa - \epsilon_r & \xrightarrow{\quad} & \kappa = \lambda - \epsilon_{r+1} \end{array}$$

It turns out that in this case columns  $k$ ,  $k + 1$  and  $k + 2$  cannot be shape equivalent to a triangle in both fillings. We first observe that this would force  $u = r + 1$ : if  $u < r + 1$ , columns  $k$ ,  $k + 1$  and  $k + 2$  form a row in the diagram corresponding to circles (i.e., the partitions on top), since the partitions  $\lambda - \epsilon_r - \epsilon_{r+1}$ ,  $\lambda - \epsilon_r$ ,  $\lambda$  and  $\lambda + \epsilon_u$  differ in *columns* with strictly increasing indices. Similarly, if  $u > r + 1$ , columns  $k$ ,  $k + 1$  and  $k + 2$  form a column in the diagram corresponding to crosses, because then the partitions  $\lambda - \epsilon_r - \epsilon_{r+1}$ ,  $\lambda - \epsilon_{r+1}$ ,  $\lambda$  and  $\lambda + \epsilon_u$  differ in *rows* with strictly increasing indices.

However, if  $u = r + 1$ , we have a cell

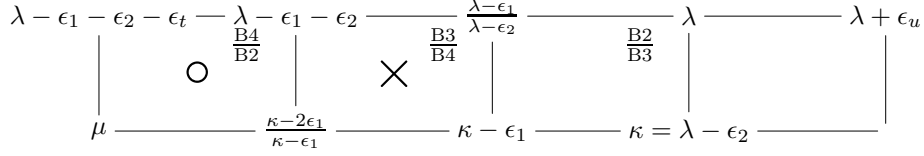
$$\begin{array}{ccc} \lambda & \xrightarrow{\quad} & \lambda + \epsilon_{r+1} \\ | & & | \\ \lambda - \epsilon_{r+1} & \xrightarrow{\quad} & \end{array}$$

which is impossible, considering the local rules.

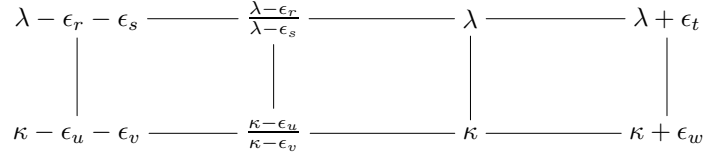
We conclude that columns  $k - 1$ ,  $k$  and  $k + 1$  must be shape equivalent to a triangle. By reasoning similar to above we find  $t = r$  and therefore  $\mu = \kappa - \epsilon_{r-1} - 2\epsilon_r$  by B3 and B2 respectively.

(f)  $\kappa = \lambda - \epsilon_s$  and  $s = r + 1$ ,  $r = 1$ .

This case is very similar to the preceding one. Again we find that  $t = r$ , and conclude that the cell in the top row and column  $k - 1$  will now contain a circle, the cell in column  $k$  a cross,  $\mu = \kappa - 2\epsilon_1$ :



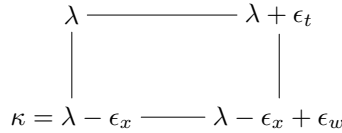
(2) Within this stage, the partitions between columns  $k - 1$  and  $k$  of the two growth diagrams differ. We show that cases in this stage can only be followed by cases of Stage 2 or 3.



This situation occurs after Case 1e and thus can only occur if columns  $k - 1$ ,  $k$  and  $k + 1$  are shape equivalent to a triangle in both fillings. Throughout this subcase, in the situation of the diagram above, we maintain  $r < t \leq s$ . Note that this condition is satisfied by the partitions along the bottom of the diagram in Case 1e. We are going to show that we also have  $u < w \leq v$  (in Cases a,b, and c) or that we continue with one of the cases of Stage 3.

(a)  $\kappa = \lambda - \epsilon_x$  and  $r$ ,  $s$  and  $x$  are all different.

By B2 we obtain  $\kappa - \epsilon_u = \lambda - \epsilon_r \cap \lambda - \epsilon_x$  and thus  $u = r$ . Similarly, we have  $v = s$ . To determine  $w$ , we consider the cell

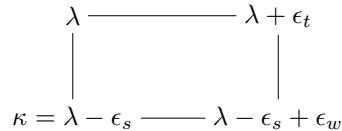


If  $w = x$ , we obtain (remember  $t > 1$ ) by B3  $x = t - 1$ . Since  $r \neq x = w$  and  $r \leq t - 1 = w$  we also have  $u = r < w = t - 1 \leq s = v$ .

If, however,  $w \neq x$ , then the local rules force  $w = t$ .

(b)  $\kappa = \lambda - \epsilon_s$ .

By B2 we obtain  $u = r$ , by B3 that  $v = s - 1$ . Now consider



If  $w = s$ , the local rules imply  $t = s + 1$ , which contradicts our assumption  $t \leq s$ . Thus,  $w \neq s$ , which entails  $w = t$ . Since  $t = s$  is impossible by the local rules, we have indeed  $u = r < w = t \leq s - 1 = v$ .

(c)  $\kappa = \lambda - \epsilon_r$  and  $r > 1$ .

By B3 we obtain  $u = r - 1$  and by B2  $v = s$ . To determine  $w$ , we consider the cell

$$\begin{array}{ccc} \lambda & \text{-----} & \lambda + \epsilon_t \\ | & & | \\ \kappa = \lambda - \epsilon_r & \text{-----} & \lambda - \epsilon_r + \epsilon_w \end{array}$$

If  $w = r$  we immediately have  $u = r - 1 < w = r \leq v = s$ . If  $w \neq r$ , we obtain  $w = t$  and  $u = r - 1 < w = t \leq s = v$ .

(d)  $\kappa = \lambda - \epsilon_r$  and  $r = 1$ .

In this case the growth diagram looks as follows:

$$\begin{array}{ccccc} \lambda - \epsilon_1 - \epsilon_s & \text{-----} & \frac{\lambda - \epsilon_1}{\lambda - \epsilon_s} & \text{-----} & \lambda & \text{-----} & \lambda + \epsilon_t \\ | & \times & \frac{\text{B2}}{\text{B4}} & | & \frac{\text{B4}}{\text{B2}} & | & \\ \lambda - \epsilon_1 - \epsilon_s & \text{-----} & \frac{\lambda - \epsilon_1}{\lambda - \epsilon_1 - \epsilon_s} & \text{-----} & \kappa = \lambda - \epsilon_1 & \text{-----} & \lambda + \epsilon_t \end{array}$$

We are thus lead to a situation of Stage 3.

(3) In this final stage, the growth diagram is of one of the following forms:

(a)  $u \neq r$

$$\begin{array}{ccccc} \lambda - \epsilon_r & \text{-----} & \frac{\lambda}{\lambda - \epsilon_r} & \text{-----} & \lambda \\ | & & | & & | \\ \lambda - \epsilon_u - \epsilon_r & \text{-----} & \frac{\lambda - \epsilon_u}{\lambda - \epsilon_u - \epsilon_r} & \text{-----} & \lambda - \epsilon_u \end{array}$$

(b)  $r > 1$

$$\begin{array}{ccccc} \lambda - \epsilon_r & \text{-----} & \frac{\lambda}{\lambda - \epsilon_r} & \text{-----} & \lambda \\ | & & | & & | \\ \lambda - \epsilon_{r-1} - \epsilon_r & \text{-----} & \frac{\lambda - \epsilon_r}{\lambda - \epsilon_{r-1} - \epsilon_r} & \text{-----} & \lambda - \epsilon_r \end{array}$$

(c)

$$\begin{array}{ccccc} \lambda - \epsilon_1 & \text{-----} & \frac{\lambda}{\lambda - \epsilon_1} & \text{-----} & \lambda \\ | & \circ & | & \times & | \\ \lambda - \epsilon_1 & \text{-----} & \lambda - \epsilon_1 & \text{-----} & \lambda - \epsilon_1 \end{array}$$

By considering the different cases as detailed above, the reader can convince herself of the validity of the claim.  $\square$

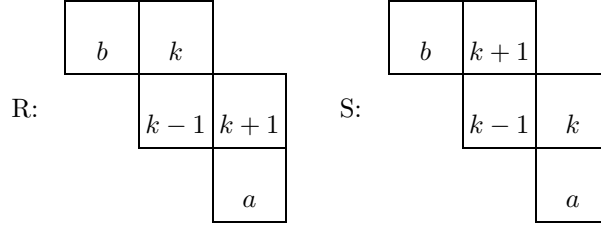
**Lemma A.4.** *Let  $R$  and  $S$  be a partial Young tableaux obtained from each other by interchanging the entries  $k$  and  $k+1$ . Suppose that the entries  $k-1$ ,  $k$  and  $k+1$  of both  $R$  and  $S$  are shape equivalent to a triangle. Then  $jdt(S)$  can be obtained from  $jdt(R)$  by interchanging entries  $k-1$  and  $k$ .*

*Similarly, suppose that  $S$  and  $R$  are obtained from each other by interchanging the entries  $k-1$  and  $k$ , and entries  $k-1$ ,  $k$  and  $k+1$  of both  $R$  and  $S$  are shape equivalent to a triangle. Then  $jdt(S)$  can be obtained from  $jdt(R)$  by either interchanging entries  $k-2$  and  $k-1$  or entries  $k-1$  and  $k$ .*

*Proof.* Consider the effect of applying the algorithm  $jdt$  to  $R$ , using the description via slides on tableaux. If the two cells whose entries differ in  $R$  and  $S$  are not

adjacent, their entries will never be compared by the algorithm. The statement then follows since  $jdt$  subtracts one from all entries of the tableau.

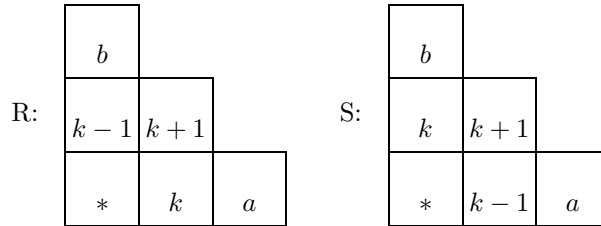
Now consider the case that  $k$  and  $k + 1$  are adjacent. We first show that the cells containing  $k - 1$ ,  $k$  and  $k + 1$  must be arranged as follows in  $R$  and  $S$ :



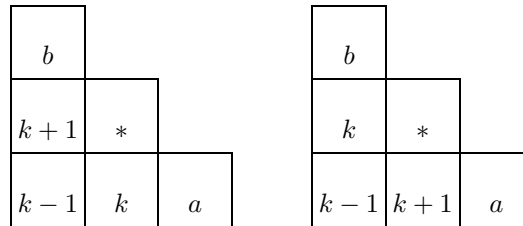
If  $k - 1$  were in a higher row, the entries 1, 2 and 3 would form a single row in  $jdt^{k-2}(R)$ . But this is incompatible with the hypothesis that they are shape equivalent to a triangle. Similarly, if  $k - 1$  were in a lower row, 1, 2 and 3 would form a column in  $jdt^{k-2}(S)$ , which again contradicts the hypothesis.

We now observe that both  $a$  and  $b$  must be smaller than  $k - 1$ , since entries in rows and columns are strictly increasing. Thus, in this case,  $jdt$  can never swap the empty cell with the cell containing  $k - 1$ . Taking into account that  $jdt$  subtracts one from all entries, we conclude that  $jdt(S)$  can be obtained from  $jdt(R)$  by exchanging entries  $k - 1$  and  $k$ .

We now consider the case that entries  $k - 1$  and  $k$  were swapped to obtain  $S$  from  $R$ , and the cells containing  $k - 1$  and  $k$  are adjacent. Then, the cells containing  $k - 1$ ,  $k$  and  $k + 1$  must be arranged as follows:



In this situation, both  $a$  and  $b$  must be greater than  $k + 1$ . Thus, if during  $jdt$  the empty cell is moved to the place marked with a  $*$  above, after two steps of the algorithm we have the following situations:



Therefore, only entries  $k$  and  $k + 1$  are exchanged. Taking into account that  $jdt$  subtracts one from all entries, we conclude that  $jdt(S)$  can be obtained from  $jdt(R)$  by exchanging entries  $k - 1$  and  $k$ . □

Let us restate Proposition 4.7 for easier reference:

**Proposition A.5.** *Consider the following two fillings:*

$$\boxed{\alpha} \boxed{\beta} \boxed{\delta} \quad \text{and} \quad \boxed{\alpha} \boxed{\gamma} \boxed{\delta}$$

and suppose furthermore that  $\beta$  and  $\gamma$  are Knuth equivalent. Then, applying  $\bar{j}$  to both fillings we obtain

$$\boxed{\alpha' | \beta' | \delta'} \quad \text{and} \quad \boxed{\alpha' | \gamma' | \delta'}$$

where  $\alpha'$  has exactly one column less than  $\alpha$  and  $\delta'$  has exactly one more column than  $\delta$ . In this situation,  $\beta'$  and  $\gamma'$  are Knuth equivalent.

Similarly, consider

$$\begin{array}{|c|} \hline \delta \\ \hline \beta \\ \hline \alpha \\ \hline \end{array} \quad \text{and} \quad \begin{array}{|c|} \hline \delta \\ \hline \gamma \\ \hline \alpha \\ \hline \end{array}$$

and suppose furthermore that  $\beta$  and  $\gamma$  are dual Knuth equivalent. Then, applying  $\bar{j}$  to both fillings we obtain

$$\begin{array}{|c|} \hline \delta' \\ \hline \beta' \\ \hline \alpha' \\ \hline \end{array} \quad \text{and} \quad \begin{array}{|c|} \hline \delta' \\ \hline \gamma' \\ \hline \alpha' \\ \hline \end{array}$$

where  $\alpha'$ ,  $\beta'$  and  $\delta'$  have as many rows as  $\alpha$ ,  $\beta$  and  $\delta$  respectively. In this situation,  $\beta'$  and  $\gamma'$  are dual Knuth equivalent.

*Proof.* We commence by proving the case of standard fillings. To prove the first statement, we observe that  $\beta$  and  $\gamma$  can be transformed one into the other using a sequence of Knuth transformations. By transitivity, we only need to consider the case where  $\beta$  and  $\gamma$  differ by a single Knuth relation. In this situation we can apply Proposition A.3 and Lemma A.4: by Proposition A.3, the upper borders of  $\beta$  and  $\gamma$  differ in a single partition, say between columns  $k$  and  $k+1$ . Therefore, the corresponding partial Young tableaux can be obtained from each other by interchanging  $k$  and  $k+1$  and we can apply Lemma A.4. It follows that the partitions labelling the upper border of  $\beta'$  and  $\gamma'$  also differ in a single position. Thus, we can apply the converse direction of Proposition A.3 to conclude that the fillings  $\boxed{\alpha' | \beta' | \delta'}$  and  $\boxed{\alpha' | \gamma' | \delta'}$  differ only by a single Knuth relation.

The second statement follows by similar reasoning directly from Proposition A.3. We only have to observe that the notions of Knuth equivalence and dual Knuth equivalence are connected by reflecting diagrams about the main diagonal.

It remains to reduce the case of arbitrary fillings to the standard case. Let  $\boxed{\bar{\alpha} | \bar{\beta} | \bar{\delta}}$  be the partial standardisation of the filling  $\boxed{\alpha | \beta | \delta}$  described in Lemma 4.6, i.e., all columns but the first of  $\alpha$  are standardised, similarly for  $\boxed{\bar{\alpha} | \bar{\gamma} | \bar{\delta}}$ . As before, we can now assume that  $\bar{\beta}$  and  $\bar{\gamma}$  differ by a single Knuth relation, and deduce that  $\boxed{\bar{\alpha}' | \bar{\beta}' | \bar{\delta}'}$  and  $\boxed{\bar{\alpha}' | \bar{\gamma}' | \bar{\delta}'}$  differ only by a single Knuth relation. By Lemma 4.6 we have  $\text{std}(\bar{j}(\boxed{\alpha | \beta | \delta})) = \text{std}(\boxed{\bar{\alpha}' | \bar{\beta}' | \bar{\delta}'})$  and  $\text{std}(\bar{j}(\boxed{\alpha | \gamma | \delta})) = \text{std}(\boxed{\bar{\alpha}' | \bar{\gamma}' | \bar{\delta}'})$ , and the claim follows.  $\square$

## REFERENCES

- [1] Jürgen Backelin, Julian West, and Guoce Xin, *Wilf-equivalence for singleton classes*, Advances in Applied Mathematics **38** (2007), no. 2, 133–148.
- [2] Giusi Castiglione and Antonio Restivo, *Reconstruction of L-convex polyominoes*, 9th International Workshop on Combinatorial Image Analysis, Electronic Notes in Discrete Mathematics, vol. 12, Elsevier, Amsterdam, 2003, p. 12 pp. (electronic).
- [3] William Y. C. Chen, Eva Y. P. Deng, Rosena R. X. Du, Richard P. Stanley, and Catherine H. Yan, *Crossings and nestings of matchings and partitions*, Transactions of the American Mathematical Society **359** (2007), no. 4, 1555–1575 (electronic), math.CO/0501230.
- [4] William Y.C. Chen, Svetlana Poznanović, Catherine H. Yan, and Arthur L.B. Yang, *Major index for 01-fillings of moon polyominoes*, Preprint (2009), math.CO/0902.3637.
- [5] Anna de Mier, *k-noncrossing and k-nonnesting graphs and fillings of Ferrers diagrams*, Combinatorica **27** (2007), no. 6, 699–720, math.CO/0602195.

- [6] Myriam de Sainte-Catherine and Gérard Viennot, *Enumeration of certain Young tableaux with bounded height*, Combinatoire énumérative (Montreal, Que., 1985/Quebec, Que., 1985), Lecture Notes in Mathematics, vol. 1234, Springer, Berlin, 1986, pp. 58–67.
- [7] Sergi Elizalde, *A bijection between 2-triangulations and pairs of non-crossing Dyck paths*, Journal of Combinatorial Theory, Series A **114** (2007), no. 8, 1481–1503, math.CO/0610235.
- [8] Sergey Fomin, *The generalized Robinson-Schensted-Knuth correspondence*, Zapiski Nauchnykh Seminarov Leningradskogo Otdeleniya Matematicheskogo Instituta imeni V. A. Steklova Akademii Nauk SSSR (LOMI) **155** (1986), no. Differentsialnaya Geometriya, Gruppy Li i Mekh. VIII, 156–175, 195.
- [9] Sergey V. Fomin, *Duality of graded graphs*, Journal of Algebraic Combinatorics **3** (1994), no. 4, 357–404.
- [10] ———, *Schensted algorithms for dual graded graphs*, Journal of Algebraic Combinatorics **4** (1995), no. 1, 5–45.
- [11] Curtis Greene, *An extension of Schensted's theorem*, Advances in Mathematics **14** (1974), 254–265.
- [12] Jakob Jonsson, *Generalized triangulations and diagonal-free subsets of stack polyominoes*, Journal of Combinatorial Theory, Series A **112** (2005), no. 1, 117–142.
- [13] Jakob Jonsson and Volkmar Welker, *A spherical initial ideal for Pfaffians*, Illinois Journal of Mathematics **51** (2007), no. 4, 1397–1407, math.CO/0601335.
- [14] Anisse Kasraoui, *Ascents and descents in 01-fillings of moon polyominoes*, European Journal of Combinatorics (2009), math.CO/0812.0799.
- [15] Christian Krattenthaler, *Growth diagrams, and increasing and decreasing chains in fillings of Ferrers shapes*, Advances in Applied Mathematics **37** (2006), no. 3, 404–431, math.CO/0510676.
- [16] Carlos M. Nicolás, *Another bijection between 2-triangulations and pairs of non-crossing Dyck paths*, Proceedings of the 21st International Conference on Formal Power Series and Algebraic Combinatorics, Discrete Mathematics and Theoretical Computer Science, DMTCS, 2009, pp. 699–710.
- [17] Astrid Reifegerste, *Permutation sign under the Robinson-Schensted correspondence*, Annals of Combinatorics **8** (2004), no. 1, 103–112.
- [18] Tom Roby, *Applications and extensions of Fomin's generalization of the Robinson-Schensted correspondence to differential posets*, Ph.D. thesis, M.I.T., Cambridge, Massachusetts, 1991.
- [19] Tom Roby, Frank Sottile, Jeff Stroomer, and Julian West, *Complementary algorithms for tableaux*, Journal of Combinatorial Theory, Series A **96** (2001), no. 1, 127–161, math.CO/0002244.
- [20] Bruce E. Sagan, *The symmetric group*, Wadsworth & Brooks/Cole, Pacific Grove, California, 1987.
- [21] Richard P. Stanley, *Enumerative combinatorics. Vol. 2*, Cambridge Studies in Advanced Mathematics, vol. 62, Cambridge University Press, Cambridge, 1999, With a foreword by Gian-Carlo Rota and appendix 1 by Sergey Fomin.

INSTITUT FÜR ALGEBRA, ZAHLENTHEORIE UND DISKRETE MATHEMATIK, LEIBNIZ UNIVERSITÄT HANNOVER, WELFENGARTEN 1, D-30167 HANNOVER, GERMANY

*E-mail address:* martin.rubey@math.uni-hannover.de

*URL:* <http://www.iazd.uni-hannover.de/~rubey/>